Bonding and elementary steps in catalysis

Document status and date:
Published: 01/01/1993

Document Version:
Publisher's PDF, also known as Version of Record (includes final page, issue and volume numbers)

Please check the document version of this publication:

• A submitted manuscript is the version of the article upon submission and before peer-review. There can be important differences between the submitted version and the official published version of record. People interested in the research are advised to contact the author for the final version of the publication, or visit the DOI to the publisher's website.
• The final author version and the galley proof are versions of the publication after peer review.
• The final published version features the final layout of the paper including the volume, issue and page numbers.

Link to publication

Download date: 04. Oct. 2023

Chapter 4

Bonding and elementary steps in catalysis

4.1 INTRODUCTION

In this chapter we discuss the bonding to transition metal elements and the elementary reactions that can occur in transition metal complexes and on surfaces of solids. The bonding will be discussed in Section 4.2 in terms that are applicable to both homogeneous and heterogeneous catalysts, the emphasis being on what they have in common and what distinguishes them. Section 4.3 gives a summary of the organometallic reactions that are important as elementary steps in homogeneous catalysts; working with this 'basis set' it is in many cases possible for the reader to write down a likely mechanism for a reaction for which only the overall formula is known. In part these reactions are also relevant to heterogenous catalysis and this section forms a good introduction to the next, Section 4.4, which deals with reactions on metal surfaces and solid acids. It will be very instructive to compare the steps of the organometallic complexes with the new possibilities created by the metal and oxide surfaces. In passing, we have also tried to point out the differences existing in the vocabulary between the homogeneous schools and the heterogeneous schools in catalysis. We do not propose that unique meanings can be attached to the words used, but it is necessary, and hopefully sufficient, that the reader is made aware of these minor obstacles.

4.2 BONDING

4.2.1 Bonding to Transition Metal Surfaces

The valence electron distribution of a transition metal surface is sketched in Fig. 4.1. A narrow d valence electron band is overlapped by a broad s–p valence

electron band. Per atom, the number of electrons in the s,p valence electron band can be considered to be constant and equal to 1. The s character of the atomic orbitals dominates in this valence band. The d valence electron content varies. For the metals Cu, Ag and Au the d valence electron band is completely occupied. When one moves from right to left in a row of the periodic system, the d valence electron occupation of the metal decreases. In Ni, Pd and Pt the d valence electron occupation is 9, etc. The width of the d valence electron band increases when moving down in a column of the periodic system or to the left, moving along a row. For a metal (i.e. the solid) the ionization potential is less than for an atom (the resulting positive charge is screened in the bulk metal) and is called the work function. The work function (E_F) decreases when moving from right to left along a row, and increases when moving downward along a column in the periodic system. The d atomic orbitals have a smaller spatial expansion than the s atomic orbitals, which explains the smaller width of the d valence atomic orbitals.

The bond strength to transition metal surfaces decreases with increasing d valence electron occupation. It tends to decrease when moving downward along a column of the periodic system. The metal–metal bond strength becomes larger because the metal electrons become more delocalized due to the larger orbital overlap. Upon chemisorption electrons have to localize on the surface involved in the chemisorptive bond. The larger the delocalization of the metal electrons, the higher is the cost involved in localization of the electrons and the smaller the chemisorptive bond energy. In addition the work function tends to increase, resulting in a decrease of polarity of the adatom (adsorbed atom) surface chemical bond. For instance carbon, oxygen and hydrogen atoms are bonded more strongly to Ni
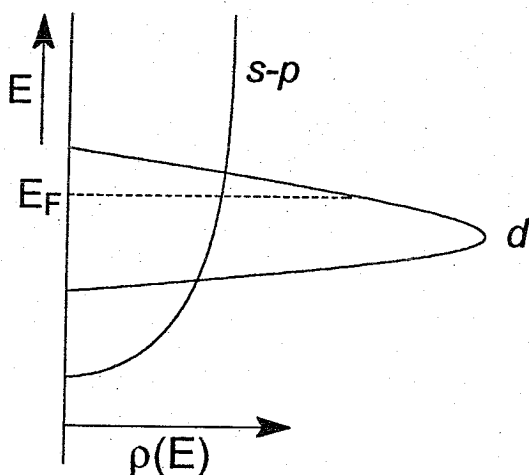

Fig. 4.1. The valence electron distribution at a transition metal surface (schematic).

than to Pt. Exceptions to this rule exist, however. For example CO binds more strongly to Pt than to Ni, but O_2 and N_2 show the expected, reverse behaviour. The angular dependence of d atomic orbitals is of relevance when orbital symmetry arguments are important. This will become especially apparent in Section 4.4 where association and dissociation reactions will be discussed [1,2].

Generally, the bonding of adatoms other than hydrogen to a metal surface is highly coordination-dependent, whereas molecular adsorption tends to be much less discriminative. For the different metals the bond strength of an adatom also tends to vary much more than the chemisorption energy of a molecule. Atoms bind more strongly to surfaces than molecules do. Here we will discuss the quantum chemical basis of chemisorption to the transition metal surfaces. We will illustrate molecular chemisorption by an analysis of the chemisorption bond of CO [3] in comparison with the atomic chemisorption of a C atom.

The valence electron orbitals and energies of CO and C are sketched in Fig. 4.2. In a molecule, atomic orbitals form bonding and antibonding orbitals, separated by an energy gap. In CO the highest occupied molecular orbital, the 5σ orbital is σ symmetric with respect to the molecule's axis. It is separated by approximately 7 eV from the lowest two unoccupied degenerate $2\pi^*$ orbitals, of π symmetry with respect to the molecule's axis. The unoccupied $2\pi^*$ orbitals are antibonding and result from the interaction between the C_{p_x} and O_{p_x} and C_{p_y} and O_{p_y} orbitals. In the atom, atomic p orbitals are partially occupied, separated by approximately 20 eV from the doubly occupied $2s$ atomic orbital. CO adsorbs perpendicular to the transition metal surface, attached via its carbon atom. When adsorbed atop the surface valence s-electrons will interact with the 5σ orbital, but their interaction is symmetry forbidden with the p-symmetric $2\pi^*$ orbitals.

Interaction of π-type CO orbitals with the s valence atomic orbitals is only possible in high coordination sites (in the organometallic nomenclature these are called bridging sites, denoted μ (or μ_2), μ_3, and μ_4 for sites involving 2, 3 and 4 metal atoms, respectively). As illustrated in Fig. 4.3 they can then interact with asymmetric group orbitals that are linear combinations of atomic s orbitals of the surface atoms.

When CO is adsorbed atop (monometallic, end-on), the π-type CO $2\pi^*$ orbitals will interact with the symmetric metal d atomic orbitals as well as p_x or p_y orbitals. The 5σ orbital will interact with d_{z^2} as well as s and p_z metal atomic orbitals. To illustrate the formation of the surface chemical bond, the interaction scheme of bond formation between the CO valence orbitals (5σ and $2\pi^*$) and metal d valence electrons is sketched in Fig. 4.4. Both bonding and antibonding orbital fragments are formed. Bonding π-type fragment orbitals are occupied. They are mainly located on the metal atom. Bonding as well as antibonding σ-type surface fragment orbitals become occupied. The σ-type bonding (σ_b) orbital fragments are mainly located on CO, the σ-type antibonding (σ_a) orbital fragments are mainly located on the metal atom.
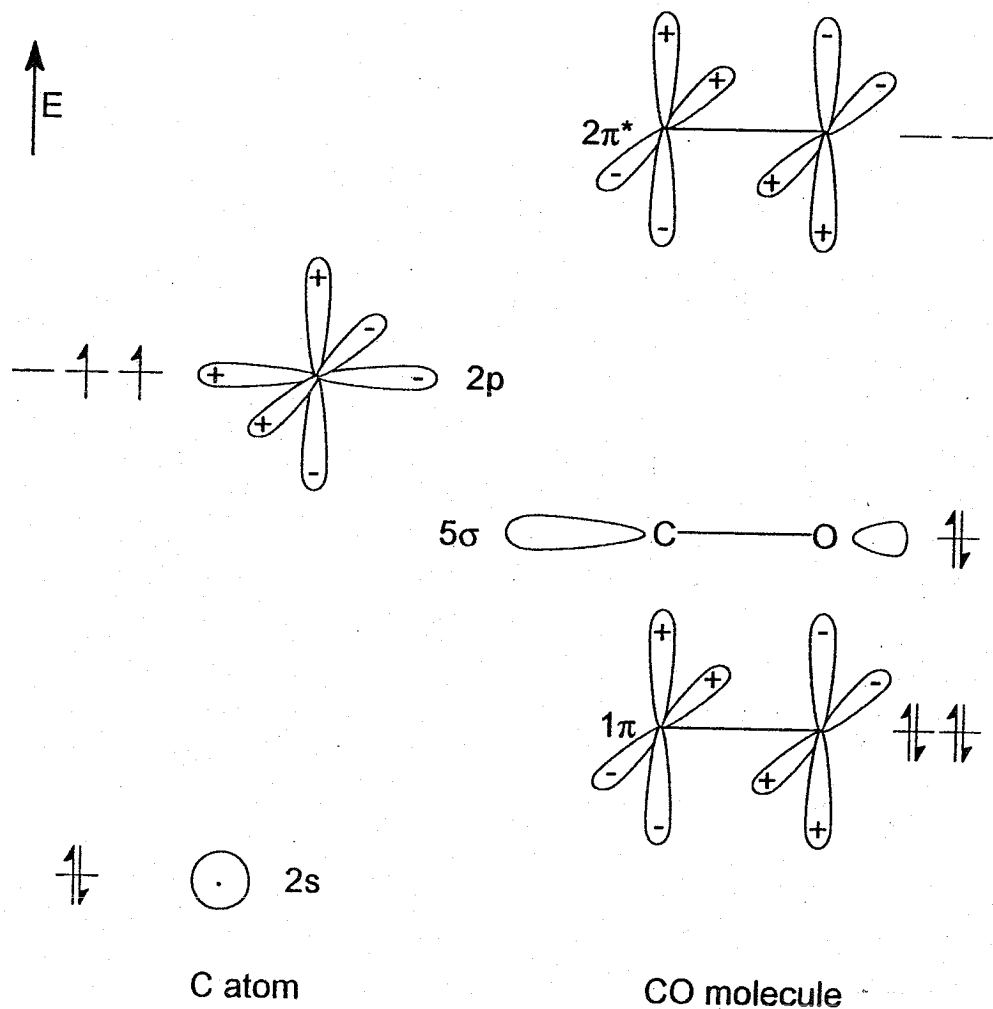
Fig. 4.2. Atomic and molecular valence electron levels.

When the d valence electron band is nearly completely filled, interaction with the doubly occupied CO 5σ orbital, leading to a significant fraction of occupied antibonding orbital fragments σ_a between adsorbate and surface atoms, will be repulsive. This Pauli repulsion is proportional to the number of surface atom neighbours and hence is a minimum in atop coordination. This counteracts the interaction with the $2\pi^*$-CO molecular orbitals, which favours high coordination
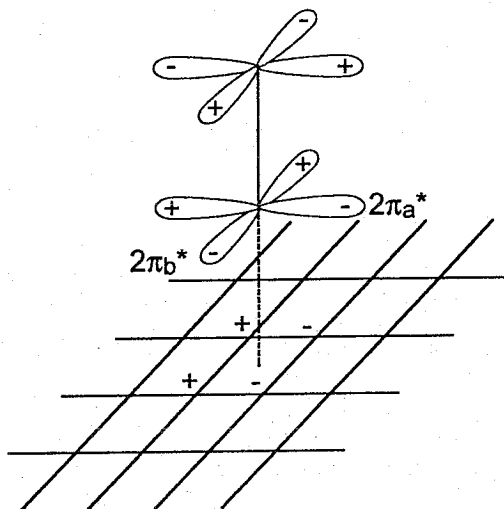
Fig. 4.3. Interaction of CO with a (100) surface in fourfold coordination. The $2\pi_a^*$ orbital interacts with the asymmetric surface group orbital $\psi_g^S = \frac{1}{2}(\varphi_a + \varphi_b - \varphi_c - \varphi_d)$.

d valence electron distribution

metal d valence atomic orbitals

CO valence electrons

Fig. 4.4. Quantum chemistry of the CO d valence electron interaction (schematic). On the left the d valence electron distribution is sketched, which is typical of a transition metal.

sites. Different from the CO 5σ orbital, the energy of the unoccupied $2\pi^*$ orbitals is higher than the metal surface Fermi energy.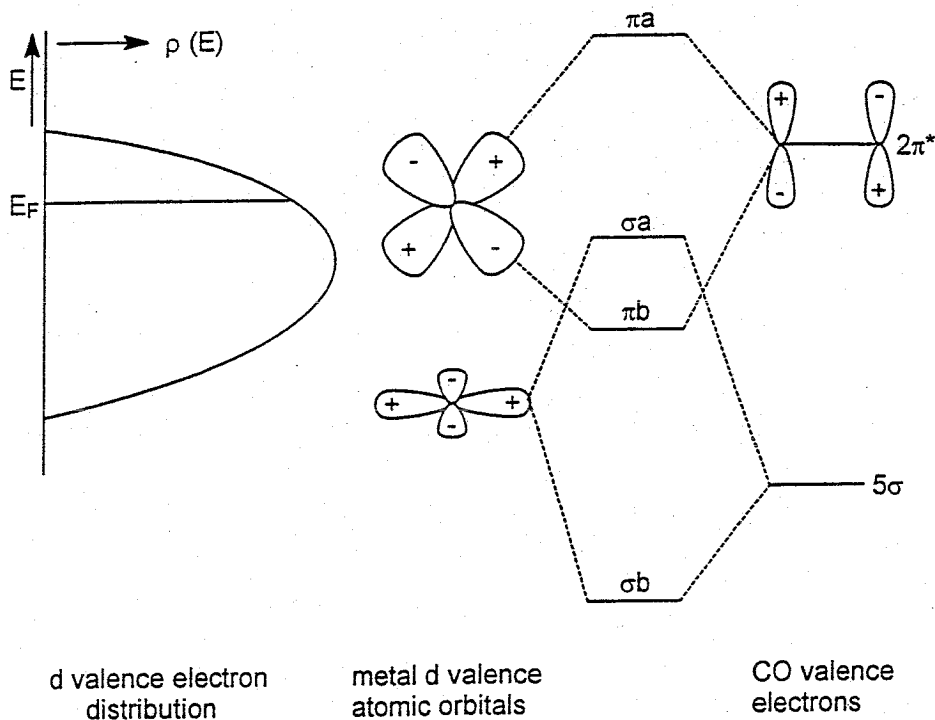 The occupied orbital fragments resulting from the interaction with the metal surface are mainly of bonding nature and are located on the metal surface atoms. Occupied bonding orbital fragments favour adsorption in high coordination sites.

A decrease in the d valence electron occupation decreases the occupation of the bonding π-type orbitals. This decreases the interaction energy. For the σ-type symmetric orbital fragments a decrease in electron occupation depletes antibonding orbital fragments, which results in an increase of the interaction energy. Changes in the interaction of π- and σ-type orbitals give a counteracting contribution to the overall bond strength.

Bonding between occupied adsorbate orbitals and the surface (the σ-type interaction in the case of CO chemisorption) is also referred to as electron donation. The electron occupation of the CO 5σ orbital is depleted in comparison with its occupation in the free CO molecule. Similarly, the interaction with adsorbate orbitals, which are unoccupied before adsorption (for instance the CO $2\pi^*$ orbitals of CO), is called back donation because of the increase in electron density in the CO $2\pi^*$ orbital upon bond formation. The increase is proportional to the $2\pi^*$ orbital participation in the occupied surface fragment orbitals. The $2\pi^*$ electron occupation increases with coordination. Because of the antibonding nature of the $2\pi^*$ orbital with respect to the CO bond energy, electron population of the $2\pi^*$ orbital weakens the CO bond strength. This is observed in IR spectroscopy by a decreasing frequency of the CO stretching mode. The description of surface chemical bonding in terms of electron donation and back donation is called the Blyholder model. As we will discuss in the next section it is very similar to the Chatt–Dewar–Duncanson chemical bonding model in transition metal complexes.

Bonding of the C atom to the transition metal surface is dominated by interaction with the three low-lying $2p$ C atomic orbitals. The p atomic orbitals parallel to the metal surface can only interact with the s valence orbitals in high-coordination sites. This interaction is much stronger than the corresponding CO interaction (the $2\pi^*$ orbitals should be compared), because of the lower energy of the atomic orbitals. Also these C p atomic orbitals are not part of a molecular orbital as in CO, which increases orbital overlap significantly. The overlap of the $2\pi^*$ orbital with a surface group orbital ψ_g is given by:

$$S_{2\pi^*,\psi_g} = \int (c_1 \,\psi_{p_x}^C - c_2 \,\psi_{p_x}^O) \cdot \psi_g \, d\tau \tag{4.1a}$$

$$= c_1 \int \psi_{p_x}^C \cdot \psi_g \, d\tau \tag{4.1b}$$

$$= c_1 \, S_{p_x,\psi_g} \tag{4.1c}$$

Equation (4.1c) relates the carbon p_x overlap to the overlap with a CO $2\pi^*$ orbital. The value of $|c_1|^2$ is significantly less than 1. Whereas the interaction with a molecular $2\pi^*$ orbital results only in occupied bonding orbital fragments, interaction with the atomic p_x, p_y or p_z orbitals results in a bonding orbital fragment as well as antibonding ones. This is due to the lower energy of the atomic $2p$ orbitals, as compared with molecular $2\pi^*$ orbitals.

In the atom three $2p$ orbitals are involved in the surface chemical bond. The interaction with the p_z orbital has σ symmetry with respect to the surface. Apart from an interaction with different surface symmetry orbitals and a larger overlap energy with the surface orbitals, its dependence on electron occupation is qualitatively similar to that of the p_x and p_y orbitals. Because the p_x and p_y orbitals can only interact with the surface s atomic orbitals in high coordination sites, and this bonding interaction contributes significantly to the total surface bond energy, bonding to high coordination sites is favoured.

The covalent interaction with the adatom $2p$ orbitals increases with decreasing surface d valence electron occupation, because fewer antibonding orbital fragments then become occupied. The adsorption energy of atoms varies much more strongly with d valence electron occupation than that of molecules because compensating effects occur in the surface chemical bond of molecules. As we discussed above for CO, variation in the interaction with the 5σ orbital is partially compensated for by changes in the interaction with the $2\pi^*$ orbital.

In general, therefore, high coordination sites are favoured when adsorbates interact that have partially occupied p or π type orbitals [4]. This is typically the case for most adatoms. The interaction of s or σ type orbitals with partially filled metal valence orbitals usually also shows a preference for high coordination sites. When the interaction with d valence orbitals dominates atop adsorption is favoured in group 8–11 metals. Hydrogen atoms will adsorb in high coordination sites as long as their interaction with the d valence electrons is small. This generally appears to be the case. Methyl fragments adsorbed to the Ni surface tend to favour high coordination sites [5]. The CH_3 fragment mainly interacts via its σ-symmetric lone-pair orbital. For a transition metal like Pt, with spatially more extended d atomic orbitals, one expects the methyl radical to show less preference for high coordination sites and to adsorb strongly atop [6,7]. Chemisorption of ammonia to a metal surface also occurs mainly by way of its σ type lone-pair orbital. Calculations show that on Cu, with a completely filled d valence electron band, NH_3 adsorbs preferentially atop. Bonding with the CH_3 radical or ammonia occurs mainly by the electron donating interaction with their highest occupied molecular orbital (HOMO), the σ orbital, because of the weak interaction with their lowest unoccupied molecular orbital (LUMO), which has an unfavourably high energy.

Often, as we saw for CO, interaction with HOMO as well as LUMO type adsorbate orbitals is important. This is also the case for a molecule like ethylene.
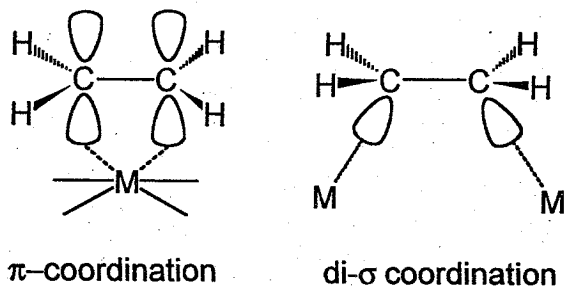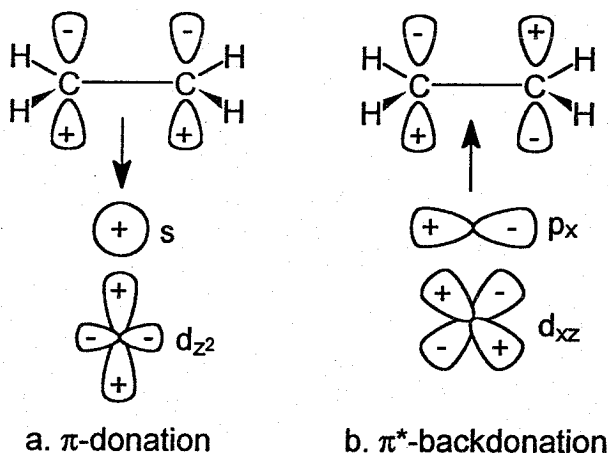
Fig. 4.5. Coordination of ethylene.

a. π-donation   b. π^*-backdonation

Fig. 4.6. Chatt–Dewar–Duncanson chemical bonding scheme of chemisorbed ethylene.

This can coordinate in two ways to the transition metal surface, namely in π coordination or di-σ coordination (Fig. 4.5) (η^2 and μ-η^1:η^1, respectively). (η^n denotes a ligand bonded with n atoms to the metal.)

The chemical bonding of π coordinated ethylene is very similar to the Chatt–Dewar–Duncanson picture of coordination (Fig. 4.6). The donating orbital is the doubly occupied π orbital that is σ-symmetric with respect to the normal to the surface. When adsorbed atop it interacts with the highly occupied d_{z^2} surface atomic orbital and the partially filled s and p_z orbitals. The ethylene LUMO is the empty asymmetric π^* orbital, which interacts with the surface d_{xz} and p_x orbitals. The corresponding overall interaction is relatively weak and no hybridization on ethylene is assumed to occur. The orbital interaction diagram of the occupied ethylene π orbital with surface atom d_{z^2} orbital is analogous to that sketched for the CO 5σ orbital in Fig. 4.4. When this d_{z^2} becomes nearly completely occupied, as occurs, for instance, for Pd or Pt, the ethylene-π surface-atom-d_{z^2} interaction

becomes repulsive. Because the spatial extension of Pt d atomic orbitals is larger than those of Pd or Ni, the repulsive interaction is largest for Pt. In order to overcome this repulsive interaction ethylene rehybridizes on Pt and adsorbs in di-σ coordination, as sketched in Fig. 4.5b (μ–η^1:η^1). The orbitals on the C atom of ethylene rehybridize from sp_2 to sp_3 hybridization, as in ethane. The CH bonds bend away from the surface and two lone pair orbitals, one in each carbon atom, develop along the missing CH bonds. They are directed towards the surface metal atoms. Ethylene now prefers coordination to two surface metal atoms [8]. Chemisorption controlled by ad-molecule hybridization generally appears to be important when the interaction with highly occupied surface d valence atomic orbitals dominates. On Pt CH_3 adsorbs atop but CH_2 adsorbs in twofold position (μ, without the subscript 2) and CH in threefold position (μ_3). On Ni, with a relatively unimportant d valence orbital interaction, all three molecule fragments prefer high coordination [9].

When surface atoms participate in more open surfaces, their average coordination number decreases, resulting in an increase of coordinative unsaturation. The width of the valence band electron density is related to the coordination number of the metal atoms. The larger the coordination number, the larger is the number of metal–metal bonds per atom, and the electrons have to be shared over more bonds. This increases the degree of delocalization of the surface electrons, which is reflected in an increased valence electron bandwidth. Because the total electron density per atom remains constant, an increased bandwidth implies a decreased average electron energy density. As is illustrated in Fig. 4.7, the electron density decreases with decreasing coordinative unsaturation in the centre of the valence electron band. This is because the integrated density is constant.

As a result, the interaction of adsorbate orbital and surface orbitals is largest for surface atoms that have the lowest surface metal atom coordination number. The bonding orbital surface fragment has a larger downward shift and the antibonding orbital fragments shift more upward. For the situation sketched in Fig. 4.7, fewer antibonding orbital fragments become occupied for the coordinatively most unsaturated atoms. This, in combination with the larger downward shift of the bonding orbital fragments, results in a stronger interaction with the coordinatively most unsaturated surface atoms. A similar overall result can be derived when empty adsorbate orbitals interact, forming only occupied bonding surface orbital fragments.

Changes in bond strength with variation of coordinative unsaturation of surface atoms are very similar to the effects of coadsorption [11]. When two adsorbate atoms share a bond with the same surface atoms, the surface atom effectively has an increased coordination number. Therefore the adatom bond strength is weaker than when there is no sharing between metal surface atoms. The heat of adsorption generally decreases at high adsorbate surface coverage as a result of this effect.
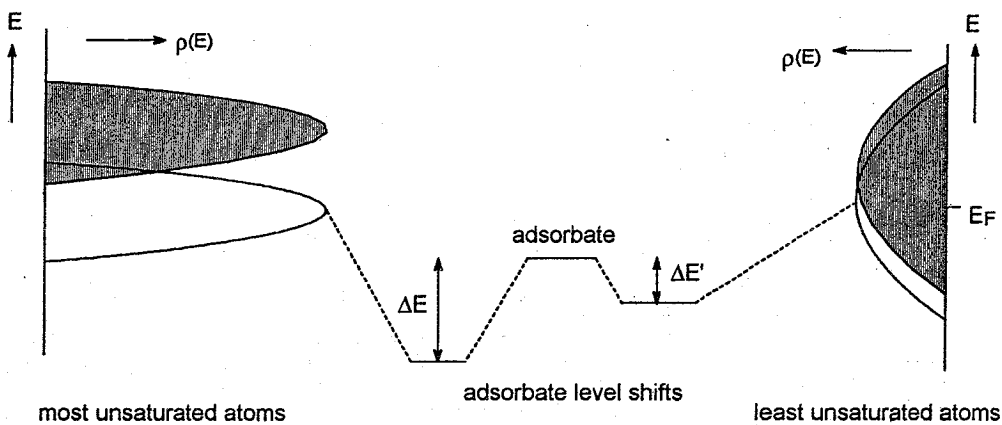
local density of states before adsorption
local density of states after adsorption

Fig. 4.7. Interaction of adsorbate orbital with surface atoms of different coordination number.
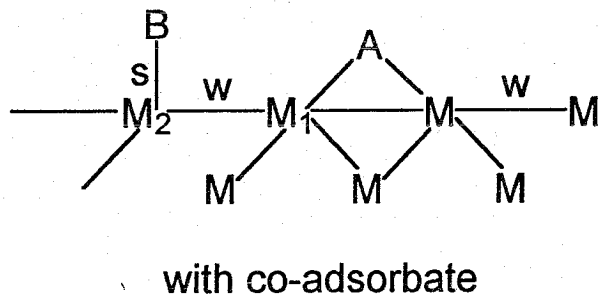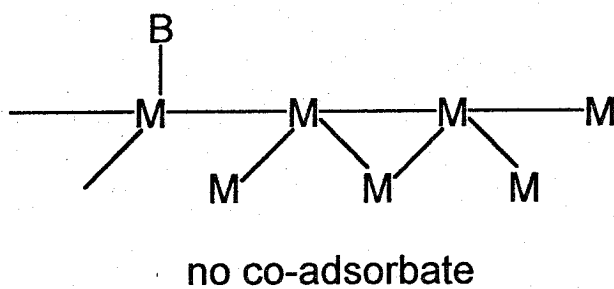

no co-adsorbate

with co-adsorbate

Fig. 4.8. Change in bond strength with a surface atom by a coadsorbate in the second coordination shell with respect to adsorbate (schematic). w = bond weakening, s = bond strengthening.

On the adsorption of strongly interacting surface atoms, in particular, the neighbouring metal–metal bonds between surface metal atoms weaken strongly. The surface–adatom interaction enhances the total number of surface atom neighbour atoms. The delocalization of the surface electrons increases, which results in a decrease of bond strength between the other atoms. This also holds for the interaction between the surface metal atoms. An alternative way of viewing this is the concept of conservation of bond order [10]. The bond order of a chemical bond is a measure of its bond strength. To a very good approximation the sum of the bond orders of the chemical bonds with a single atom is a constant. Because the total bond order per metal surface atom is conserved, an increase in coordination number decreases the bond order per bond, and hence the bond strength of the atom bonds.

The effect on the bond strength of a coadsorbate adatom B, adsorbed in the second coordination shell with respect to adatom A, is an increase of the bond energy (see Fig. 4.8). The weakened interaction between metal atoms 1 and 2, results in an increase of the M–B bond strength.

4.2.2 Chemical Bonding in Organometallic Coordination Complexes and on Surfaces of Transition Metal Compounds

Ligands and molecules bind to organometallic and coordination complexes with energies comparable to the adsorption energies found for surfaces. As on surfaces, the chemical bond formed in such complexes also contains significant s or p character. A major difference with metal surfaces is the importance of discrete valence electron occupation numbers on complex stability. A prototype coordination compound is $Ni(CO)_4$.

Figure 4.9 shows a schematic illustration of the chemical bonds of tetrahedral $Ni(CO)_4$. Bonding can be best understood by initially ignoring the (weak) interaction between Ni and CO $2\pi^*$ electrons. The interaction is dominated by the CO 5σ and Ni $4s$ and $4p$ electrons. Four approximately sp^3 hybridized orbitals are formed, directed to the four CO 5σ orbitals. Eight new orbitals, four bonding and four antibonding, are formed separated by an energy gap $2\Delta_L$.

The atomic d orbitals interact only weakly with the CO molecular orbitals. The atomic d orbitals that have orbital lobes directed to the CO ligand positions acquire an antibonding character. A small splitting ΔE_L of the d orbitals results. Electron counting shows that 18 electrons give a stable complex. In that case the five d orbitals and four bonding sp^3 orbitals are occupied. The next electron has to be placed in the highly antibonding s,p-type orbitals. This is a very general principle in the bonding of transition metal complexes. Compounds are stable as long as no antibonding orbitals become occupied. For Co, one finds that since it has one electron fewer than Ni, $Co(CO)_4$ can accept one additional electron. This
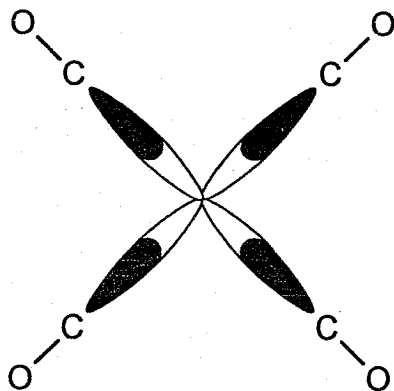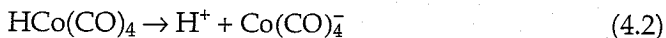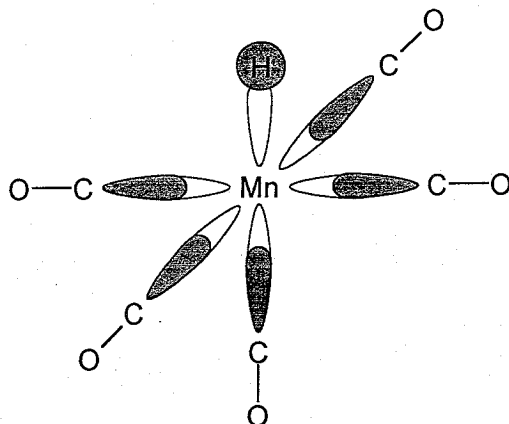
a. Hybridization orbital interaction scheme
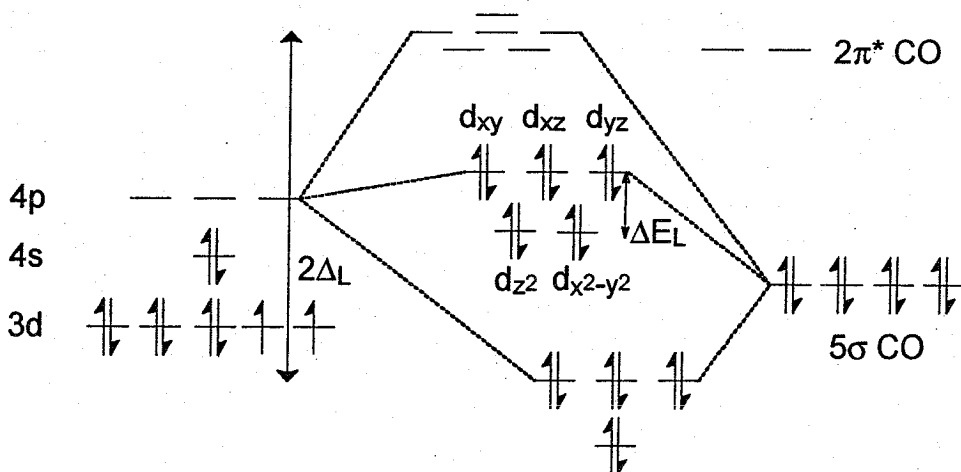
b. Molecular orbital scheme

Fig. 4.9. Chemical bonding in $Ni(CO)_4$.

is the reason why dimerization occurs giving $[Co(CO)_4]_2$, but bonding with hydrogen can also occur. Because of the stability of the $Co(CO)_4$ anion, the hydrogen atom in the hydrogen cobalt carbonyl complex has an acidic character.

$$HCo(CO)_4 \rightarrow H^+ + Co(CO)_4^- \qquad (4.2)$$

A covalent metal hydride bond is formed in $HMn(CO)_5$: its bonding scheme is shown in Fig. 4.10. Manganese has seven valence electrons: the H atom donates one electron. Again, bonding with CO is considered to occur mainly with the CO

a. Hybridization orbital scheme
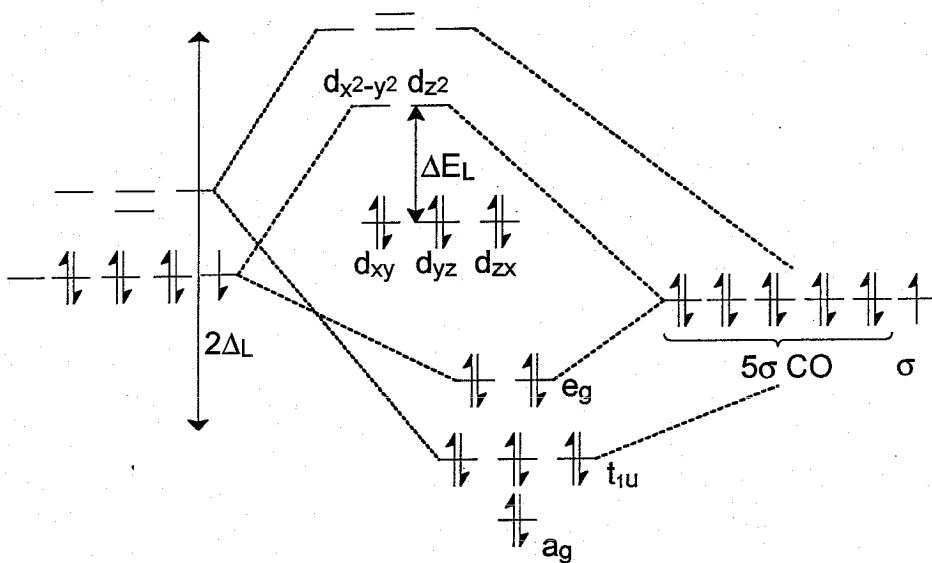
b. Molecular orbital scheme

Fig. 4.10. Chemical bonding in $HMn(CO)_5$.

5σ orbitals. Because the 5σ CO orbitals participate in bonding occupied complex orbitals and antibonding unoccupied orbitals, the electron occupation of the CO 5σ orbitals is found to decrease. Electron back donation occurs between the doubly occupied d_{xy}, d_{yz} and d_{zx} atomic orbitals and empty CO $2\pi^*$ orbitals. The d orbitals shift slightly downwards and the CO $2\pi^*$ orbitals shift slightly upwards

due to this interaction. This is the Chatt–Dewar–Duncanson picture of chemical bonding, which we discussed earlier in the context of the surface chemical bond [12]. In addition to Mn s and p electrons, the atomic $d_{x^2-y^2}$ and d_{z^2} also become involved in the bonding and antibonding orbitals formed with the CO 5σ orbitals.

A large splitting occurs between the d atomic orbitals on Mn. The d_{z^2} and $d_{x^2-y^2}$ orbitals are part of the six antibonding orbital combinations with the CO 5σ orbitals. A stable complex is formed once again with an electron count of 18. More electrons would occupy the antibonding $d_{x^2-y^2}$ and d_{z^2} orbitals, weakening the complex. The hybridized bond orbitals formed here can be considered as d^2sp^3 hybrids. A strong MnH orbital is formed. When the M-H fragment dissociates one bonding–antibonding orbital pair is removed from the orbital scheme, Fig. 4.11. The ligand field splitting changes, too. The degeneracy of the $d_{x^2-y^2}$ and d_{z^2} orbitals disappears and the $d_{z^2} - p_z$ hybridized orbital becomes the lowest unoccupied molecular orbital, directed towards the empty ligand position of hydrogen. It contains one electron.
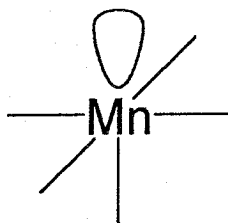
Fig. 4.11. Dangling bond orbital of Mn(CO5).

Fig. 4.12. Local cation coordination in NiO and MoS2.

The distribution of electrons over d orbitals in complexes of different geometry controls the most stable geometric configuration. This principle can also be used to understand the chemical bonding of transition metal compounds and their surfaces. We will illustrate this first by analyzing the relative stability of octahedral NiO versus trigonal prismatic MoS2.

Fig. 4.13. Orbital schemes.

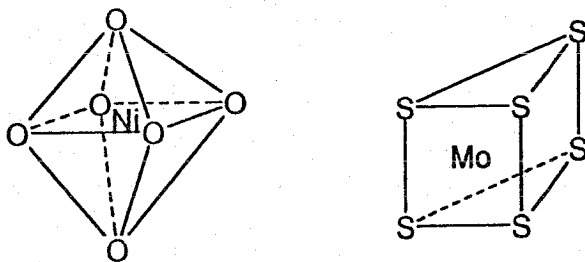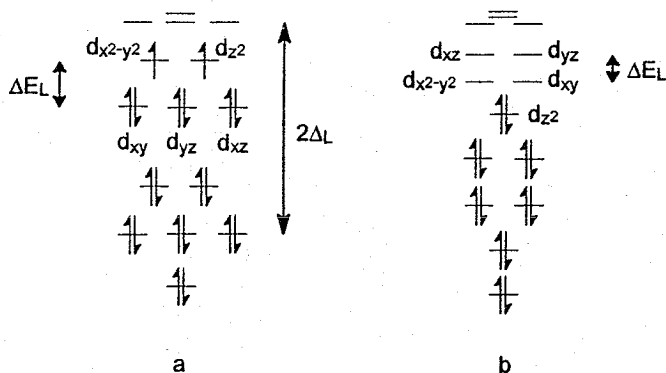Bonding in transition metal compounds can be analyzed analogously to that in transition metal complexes, by considering each oxygen or sulphur atom to contribute two electrons to the complex and an s-type orbital. The resulting orbital schemes are given in Fig. 4.13.

In NiO, the Ni^{2+} ion contributes eight electrons. Bonding is dominated by population of the bonding, mainly s,p-type, orbitals. The octahedron can be considered a 20 electron complex. Two electrons have to be placed in the bond-weakening antibonding $d_{x^2-y^2}$ and d_{z^2} orbitals. As a result of Hund's rule, this results in a triplet state. Clearly, a more stable situation exists in octahedrally coordinated Co^{3+}, forming an 18 electron complex.

When an oxygen anion is removed from a surface, a surface dangling bond appears, as described for $Mn(CO)_5$, directed towards the vacancy position. In NiO this will contain two electrons. Because it is doubly occupied, in the case of coordination to Ni^{2+} ions, interaction with the dangling bond will be weak. However for Co^{3+}, strong coordination of basic molecules containing occupied σ lone pair orbitals becomes possible.

Interestingly sulphidic compounds, having a cation coordination which is similar to that of the oxides, show large differences in their sensitivity with respect to basic molecules like NH_3. Whereas the desulphurization activity of cobalt sulphide catalysts is readily poisoned by ammonia, nickel sulphide maintains its activity to a significant extent. This agrees with the observed weak interaction of the adsorbent with the doubly occupied dangling bond orbital of the Ni^{2+} ion.

In MoS_2, which has trigonal symmetry only the nonbonding d_{z^2} orbital becomes occupied. The bond strength of MoS_2 is controlled by the occupation of bonding orbitals of low energy. Whereas, in Ni^{2+} and Co^{3+} complexes, antibonding orbitals are occupied which are also antisymmetric and able to donate electrons into antibonding adsorbate orbitals, such orbitals are not occupied in MoS_2. The corresponding surfaces are expected to behave chemically as Lewis acids.
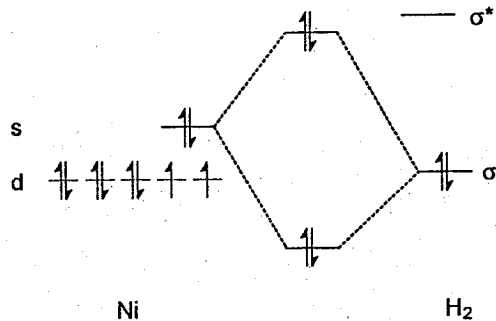
Fig. 4.14. The interaction between a Ni atom and a hydrogen molecule.

We have learned that the atomic orbitals on transition metal surfaces or in organometallic complexes are rehybridized to a significant extent. This changes the nature of the chemical bond considerably from that in the free atom. We will illustrate this by comparing dissociation of the H_2 molecule by a Ni atom and the $Ni(PH_3)_2$ complex [15–18].

In the Ni atom, the $4s$ orbital contains two electrons. This spatially extended, doubly occupied orbital experiences a large repulsive interaction with the doubly occupied H_2 σ orbital of the same symmetry. Dissociation of H_2 has a large activation energy because electron promotion has to occur from $4s$ to $3d$ atomic orbitals in order for dissociation to occur. Coordination by ligands, as in $Ni(PH_3)_2$, decreases the promotion energy. The $Ni(PH_3)_2$ complex has linear geometry (Fig. 4.15).

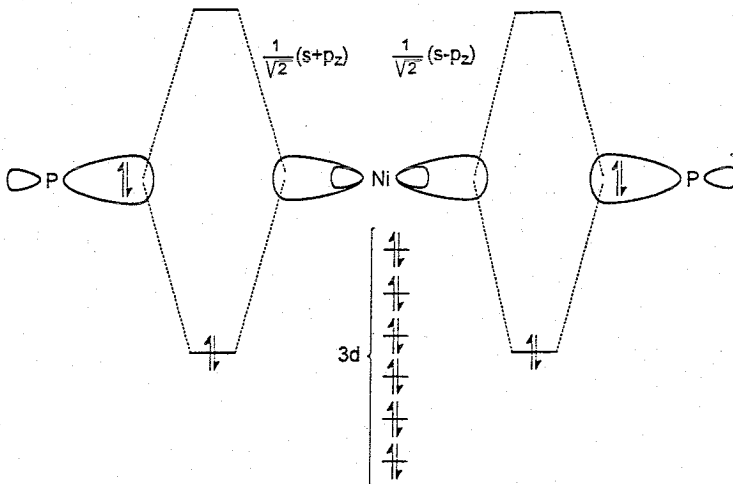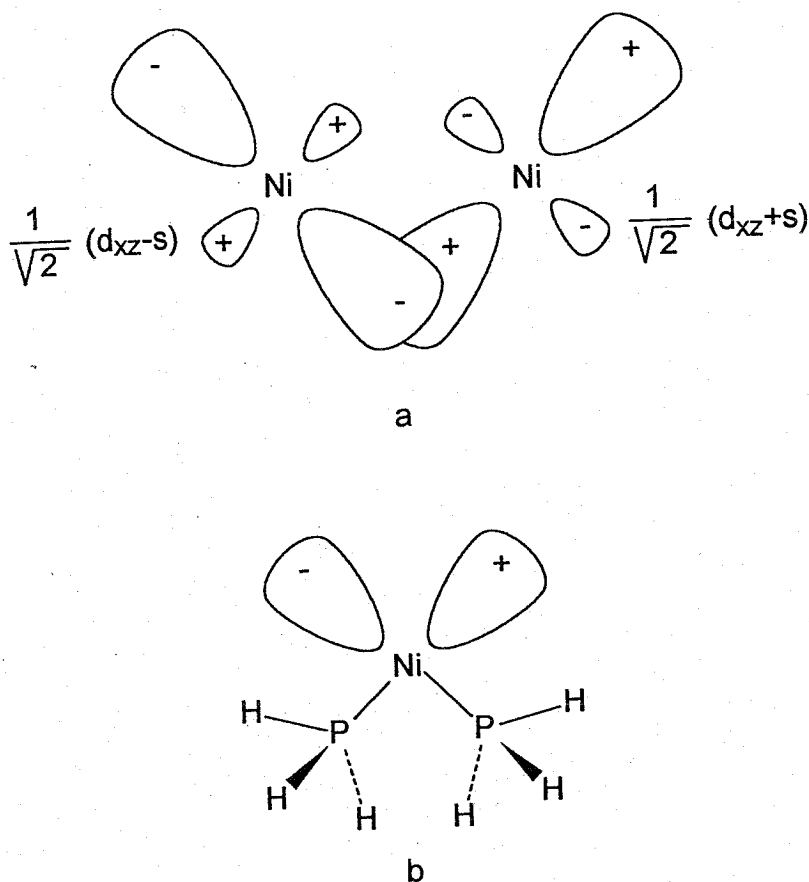Fig. 4.15. The electronic structure of $H_3P–Ni–PH_3$.

Fig. 4.16. Rehybridization of Ni atomic orbitals in the deformed Ni(PH$_3$)$_2$ complex.

Occupied bonding orbitals and non occupied antibonding orbitals between the Ni atom and the two phosphorus ligands are formed when two electrons of the Ni 4s orbitals are promoted into the Ni 3d orbitals. The Ni 4s and 4p atomic orbitals hybridize into two empty atomic orbitals directed to the occupied lone pair on the phosphorus atom. When the hydrogen molecule approaches this complex, the interaction is again weak. The empty, spatially extended Ni s-atomic type orbitals required for bonding have been pushed upwards to a high energy. Dissociation occurs only when the Ni(PH$_3$)$_2$ molecule is deformed in such a way that empty spatially extended orbitals become available.

When the H$_3$P–Ni–PH$_3$ angle becomes 90°, hybridization between the d_{xz} and s atomic orbitals, rather than s–p hybridization, results in directed orbitals suitable for coordination with the PH$_3$ ligands. In the process, empty antibonding orbitals having an s and d_{xz} nature are created, as sketched in Fig. 4.16. Their orientation and symmetry are suitable for interaction with the hydrogen molecule. Now the

antibonding H_2 σ orbital can be populated and the molecule will dissociate. Note that hybridization on the Ni atom is now d^9s^1, which is very similar to the hybridization of a Ni atom in the Ni metal surface.

When discussing the chemical bonding in $M(CO)_4$ complexes we observed that complexes become stabilized for particular electron counts. When an increase in electron count results in the population of antibonding orbitals no stable clusters are formed. An analogous rule has been formed for the stability and hence reactivity of metal clusters. It stems from the large overlap of the s and p atomic orbitals and the resulting importance of the s and p valence electrons to the cohesive energy of the metal clusters. Each atom can be considered to contribute one electron per atom to the s,p valence electron bonds of the cluster. In a closed packing geometry the clusters are approximately spherical, and hence, a stable cluster will be one with $n = 2, 8, 18$, etc. Indeed, beam experiments indicate exceptional stability or nonreactivity for such cluster atom numbers for many metals. The shell rule, however, is very approximate and in most cases it is better to consider surface atom coordination numbers when studying cluster reactivity.
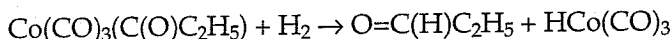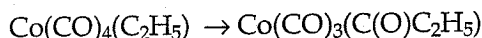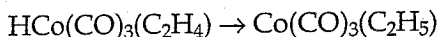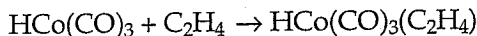

4.3 ELEMENTARY STEPS IN ORGANOMETALLIC COMPLEXES

The following paragraphs deal with the elementary steps that occur at a metal centre in a homogeneous catalytic reaction. Although the greater part of the elementary steps described have been studied in detail in model reactions of homogeneous organometallic complexes [19–23], there is general consensus that many of them can also take place at metal ions on surfaces [24]. At metallic surfaces, however, several additional reactions can take place that, by their nature, do not occur with low molecular weight, soluble organometallic complexes. The latter will be discussed in Section 4.4.

4.3.1 Creation of a Vacant Site

The function of a catalytic centre is to bring reactants together and to lower the activation barrier of their reaction. In homogeneous catalysis the catalytic centre comprises a metal centre and surrounding organic molecules. The latter molecules are called ligands and they can be neutral molecules (solvent, phosphines, CO, alkenes) or anions (e.g. halides). The ligands are usually σ donors, bringing the electron count of the complex to 18 or 16 or, especially on the left-hand-side of the periodic table, to 14 electrons, so that no electrons are forced into antibonding orbitals (see Section 4.2.2). To bring the reactants together, the metal centre must have vacant sites, i.e. it must be coordinatively unsaturated. Metal catalysis begins, we could say, with the creation of these vacant sites. In the condensed phase solvent molecules will always interact with the metal ion. The reactant

molecules are present in excess, and so may the ligands be. Therefore, a competition exists in complex formation between the desired substrate and other potential ligands present in the solution. With heterogeneous catalysts the presence of competing molecules in the gas phase controls the state of the surface. A negative order in one of the concentrations of the reactants can often be found in the expression for the rate of product formation (see the chapter on kinetics). In homogeneous catalysis this order can also be negative in ligand concentration. When the substrate coordinates strongly to the metal centre this may give rise to a zeroth order in the concentration of the substrate, i.e. Michaelis–Menten kinetics. Furthermore, coordination of the product formed during the reaction may slow down or inhibit the catalytic process. As an illustration, we may mention the cobalt-catalyzed hydroformylation reaction [25,26]:

$$HCo(CO)_4 \rightarrow HCo(CO)_3 + CO \tag{4.3}$$

$$HCo(CO)_3 + C_2H_4 \rightarrow HCo(CO)_3(C_2H_4)$$

$$HCo(CO)_3(C_2H_4) \rightarrow Co(CO)_3(C_2H_5)$$

$$Co(CO)_3(C_2H_5) + CO \rightarrow Co(CO)_4(C_2H_5)$$

$$Co(CO)_4(C_2H_5) \rightarrow Co(CO)_3(C(O)C_2H_5)$$

$$Co(CO)_3(C(O)C_2H_5) + H_2 \rightarrow O=C(H)C_2H_5 + HCo(CO)_3$$
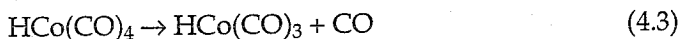
The catalyst is $HCo(CO)_4$, which must lose one molecule of CO in order to make room for an alkene molecule (Fig. 4.17).
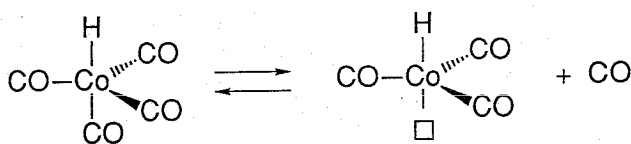
Fig. 4.17. Desorption of carbon monoxide.

A high CO pressure would shift equilibrium (4.3) to the left and the catalytic reaction would become slower. In this complex CO is a far better ligand than an alkene. On the other hand the reaction uses CO as a substrate, so it cannot be omitted. Furthermore, low pressures of CO may lead to decomposition of the cobalt carbonyl complexes to metallic cobalt and CO, which is also undesirable. Finally, the product alcohol may stabilize divalent cobalt species which are not active as a catalyst:

$$6\ ROH + 3\ HCo(CO)_4 \rightarrow Co(ROH)_6^{2+}\{Co(CO)_4^-\}_2 + 4\ CO + 1\tfrac{1}{2}\ H_2$$
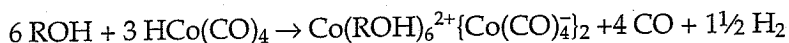
In a nutshell, we see several counteracting factors.

4.3.2 Coordination of the Substrate

The vacant site created in the required initial step of the catalytic process at the metal centre can now be occupied by the incoming substrate. Another way of looking at the question of 'creation of a vacant site' and 'coordination of the substrate' is the classical way of studying substitution reactions [27]. This is particularly useful for homogeneous complexes. Two extreme mechanisms are distinguished: a (complex) associative and a (complex) dissociative one. The discussion above concurs with the dissociative mechanism, that is to say the rate-controlling step is the breaking of the bond between the metal and the leaving ligand. In the associative process the displacement is a bimolecular process with simultaneous bond breaking and bond formation. The bond being broken or formed denotes here the bond between the reactant *molecule* and the *metal*. Note the difference in terminology between heterogeneous catalysis and coordination chemistry, the terminology adopted in homogeneous catalysis:

Homogeneous catalysis:	Meaning:	Heterogeneous catalysis:
dissociation	metal ligand bond breaking	desorption
association	metal ligand bond forming	adsorption
oxidative addition	fission of bond in substrate	dissociation
reductive elimination	making of bond giving substrate	association

In square-planar, 16-electron complexes (i.e. coordinatively unsaturated) as found for many group 9 (Co, Rh, Ir) and 10 (Ni, Pd, Pt) metals, the associative process is most common. The *trans* effect and *trans* influence ligand series [19–23] are also useful measures in the study of homogeneous catalysis. Apart from very small ligands, such as CO, H_2, and NO, steric repulsion between ligands, as well as complexes and incoming substrates, plays a dominant role in determining the kind of intermediates and complexes formed and their equilibria in solution.

Carbon monoxide and ethylene are common substrates involved in homogeneous catalysis. The bonding of carbon monoxide to a transition metal has been depicted in Fig. 4.4. The bonding of alkenes to transition metals is described by the Chatt–Dewar–Duncanson scheme involving σ donation by the filled π orbital of the alkene, and π back donation from the metal into the $π^*$ orbital of the alkene (see Fig. 4.6).

4.3.3 Insertions and Migrations

Elementary steps involving insertion or migration reactions are of prime importance for catalysis employing alkenes and carbon monoxide. Two examples taking place on a platinum centre have been depicted in Figs. 4.18 and 4.19. In these reactions an acetyl fragment is formed on the platinum centre from a coordinated CO and a methyl group. The important mechanistic difference
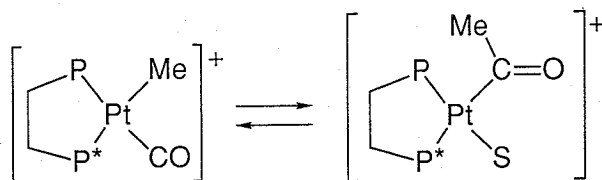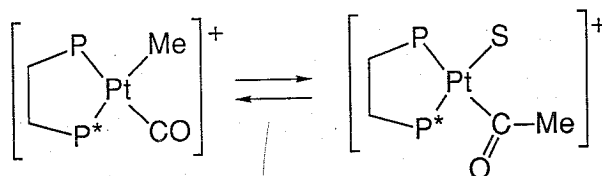
Fig. 4.18. Insertion reaction.

Fig. 4.19. Migratory insertion reaction.

between insertion and migration is that, in the insertion mechanism, CO inserts into the metal methyl bond and consequently the acyl bond formed takes the position of the former methyl group, i.e. the σ bonded fragment retains its position *trans* to P^* (Fig. 4.18). In the migration mechanism the methyl group migrates to the coordinated CO, and now the resulting acetyl group occupies the position *cis* to P^* (Fig. 4.19). There is convincing experimental evidence [28,29] (see below) in support of the migration mechanism versus the insertion mechanism, though not for the simple platinum complexes shown in Figs. 4.18 and 4.19. Results of theoretical calculations [30–32] are in better agreement with the migration mechanism, i.e. with the anionic methyl group moving to the positively charged carbon atom of carbon monoxide. Hence the most accurate description for this process is migration. In the literature, however, the reaction is usually referred to as 'insertion', perhaps mainly because the reactive unsaturated species (CO or ethene) is chosen as the linguistic subject of our sentences: 'carbon monoxide inserts giving an acyl complex'. To do justice to the intimate details of this reaction one also writes 'migratory insertion'.

So far we have automatically presumed that the reacting carbon monoxide is coordinated to the metal. For the platinum example shown that might not be an easy thing to prove, but there is experimental evidence for complexes in which methyl migration to coordinated CO occurs. The classic proof stems from a relatively inert complex in which both the migration and the exchange of coordinated CO with free CO is slow. The reaction of $CH_3Mn(CO)_5$ in the presence of ^{13}C labelled free [13]CO results in the formation of $CH_3(CO)Mn(CO)_4(^{13}CO)$ in which the labelled CO is present as carbon monoxide and not in the acetyl group (Fig. 4.20).
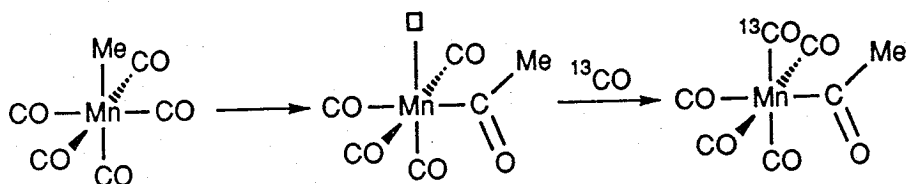
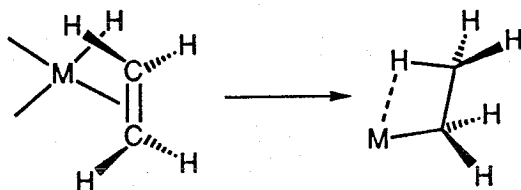Fig. 4.20. Migratory insertion to pre-coordinated CO.

Fig. 4.21. Hydride migration to ethene.

Hence there is no direct reaction between the methyl manganese unit and the newly incoming carbon monoxide. Later, when we discuss the activation of a coordinated substrate molecule toward nucleophilic attack, the latter will turn out to be an alternative for the insertion/migration process. In the reaction involving nucleophilic attack at the coordinated, activated, unsaturated substrate, the anionic fragment is an uncomplexed species. There is, as yet, no proven example of an insertion of an uncomplexed unsaturated substrate into a metal–carbon σ bond.

A second important migration reaction takes place with alkenes, rather than carbon monoxide. Figure 4.21 gives a schematic representation of a hydride that migrates to a coordinated ethene molecule *cis* to the hydride. The figure shows the hydride migration which would leave an empty space in the coordination sphere of the metal. This coordinative unsaturation can be lifted in two ways: firstly, an agostic [33] interaction with the β-hydrogens may occur; secondly, an incoming ligand may occupy the vacant site [34]. How and whether activation of a coordinated alkene takes place prior to migration is not always clear-cut. Coordinated alkenes are subject to σ donation and π back donation, and the overall outcome of the shift of electron density from and to the coordinated alkene cannot be predicted. Molecular orbital calculations [35] show that, to a simple first approximation, the coordinated alkene is not activated towards migration (i.e. nucleophilic attack) and it cannot be predicted *a priori* whether rapid migration of the hydride will occur. However, a strong polarization of the alkene will be achieved when an asymmetric bonding of the alkene is arranged, as shown in Fig. 4.22.

The migration reaction takes place in a *cis* fashion with respect to the alkene; the two atoms M and H add on the same face of the alkene (2+2 *cis*-addition). This
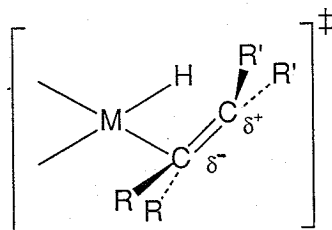
Fig. 4.22. Asymmetric coordination giving activation for nucleophilic attack.

has been unequivocally established by experiments. Later we will see reactions where this is not the case, although the overall stoichiometry is the same for both types.

Thermodynamically the insertion of an alkene into a metal–hydride bond is much more favourable than the insertion of carbon monoxide into a metal–methyl bond. The latter reaction is more or less thermoneutral and the equilibrium constant is near unity under standard conditions. The metal-hydride bond is stronger than a metal–carbon bond and the insertion of carbon monoxide into a metal hydride is thermodynamically most often uphill. Insertion of alkenes is also a reversible process, but slightly more favourable than CO insertion. Formation of new σ bonds at the cost of the loss of the π bond of the alkene during alkene hydrogenation etc., makes the overall processes of alkenes thermodynamically exothermic, especially for early transition metals.

Other insertions may involve isonitriles, alkynes, alkadienes, CO_2, and SO_2. They will not be dealt with here.

4.3.4 β-Elimination and Deinsertion

The reverse reaction of the migration of η^1-bonded anionic groups to coordinated alkenes is named β-elimination. (Compare Figs. 4.23 and 4.24).

The migration reaction diminishes the total electron count of the complex by two, and creates a vacant site at the metal; β-elimination does the opposite. β-Elimination requires a vacant site at the metal centre, and the electron count of the complex increases by two electrons during the process. The reaction resembles the β-elimination reaction occurring in many organic processes, but the difference lies in the intramolecular nature of the present process, as the eliminated alkene may be retained in the complex. In organic chemistry the reaction may well be a two-step process, e.g. proton elimination with a base followed by the leaving of the anion. In transition metal chemistry, however, it is the availability of d orbitals that greatly facilitates a concerted cis β-elimination.

Suppression of β-elimination in catalytic processes is often a desirable feature. It can be achieved in several ways, although these recommendations in many
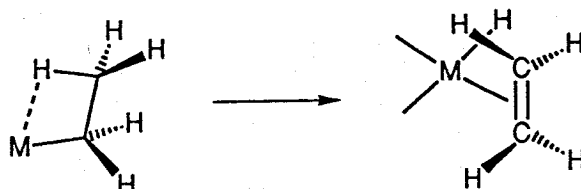
Fig. 4.23. β-Elimination.
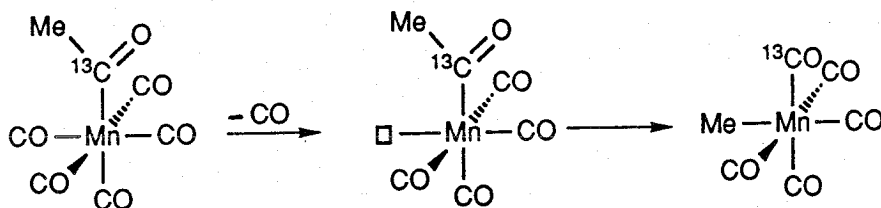
Fig. 4.24. *Cis*-deinsertion.

instances have limited practical value. Rule number one would be to avoid β-hydrogens! When carrying out a polymerization reaction with a specific alkene carrying three hydrogens this will indeed be impractical. Rule number two is to maintain coordinative saturation. Again, in a catalytic cycle this may be a counterproductive suggestion, since the next reaction in the catalytic cycle will also require a vacant site in order to bring the next substrate molecule into the coordination sphere of the metal. Thirdly, steric hindrance may hamper the correct stereochemistry required for β-elimination, and perhaps this can be used to stabilize our metal alkyl complex. The last recommendation is to seek the metals for which the metal alkyl complexes are stable with respect to the corresponding hydride/alkene metal complexes. The relative stability of metal alkyls with respect to hydrides increases for the metals on the left-hand side of the periodic table: the early transition metals and the lanthanides [36–38]. It is not surprising that the best alkene polymerization catalysts are found amongst these metals.

For metal hydride elimination from a metal alkyl (to produce an alkene) one will also find the terms 'deinsertion' and 'extrusion' rather than β-elimination. For alkenes 'β-elimination' is correct, but for CO the deinsertion nomenclature is obligatory. We have seen that insertion takes place between a σ-bonded, anionic fragment and a neutral ligand in mutual *cis* positions, as was described for the manganese complex in Figure 4.20. By the same token, the deinsertion reaction can only proceed if there is a vacant site *cis* to the acyl group. A further modification of the experiment outlined in Fig. 4.20 proves this point. A manganese acetyl complex which is ^{13}C labelled at the acyl carbonyl group was synthesized and

heated to give deinsertion of CO. The result was that the only product formed contained the methyl substituent in a position *cis* to the labelled ^{13}C, see Fig. 4.24.

4.3.5 *Oxidative Addition*

In an oxidative addition reaction an electrophilic compound XY adds to a metal complex during which the XY bond is broken and two new bonds are formed: MX and MY. X and Y are reduced, and will at least *formally* have a minus one charge and hence the *formal* oxidation state of the metal is raised by two. The coordination number of the metal also increases by two. The electron count of the metal complex increases by two, while the electron count of the metal decreases by two. Figure 4.25 gives a formal representation. Clearly, the oxidative addition will be faster when the starting metal centre is more electron rich and/or more nucleophilic and hence the reaction is promoted by electron-releasing donor atoms at the metal. The simplest form of an oxidative addition has been presented in Section 4.2.2 (Figs. 4.14–16), the reaction of nickel with dihydrogen. It has already been mentioned that both the electron count and the geometry of the coordination complex play an important role in determining the energetics of such a reaction. In the following only one popular example will be described.

The oxidative addition has been most extensively studied on iridium complexes, particularly Vaska's complex. The latter is a square planar complex, *trans*-$L_2IrCl(CO)$, with a d^8 electron count containing iridium(I). After the oxidative addition we formally obtain iridium(III), an octahedral complex, with a d^6 electron configuration; i.e. the 16-electron square-planar complex is converted into an octahedral 18-electron complex. In Fig. 4.26 we have depicted the oxidative addition of methyl iodide to Vaska's complex (L = phosphine) [39]. A large

$$L_nM^m \quad + \quad XY \quad \longrightarrow \quad L_nM^{(m+2)} \genfrac{}{}{0pt}{}{Y}{X}$$
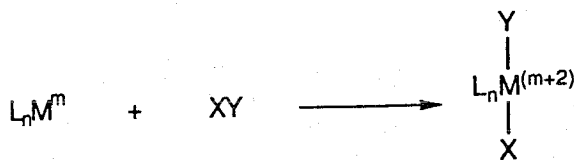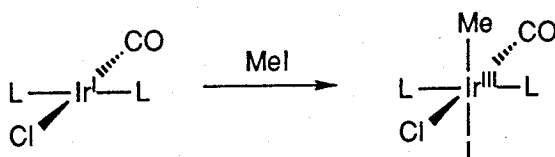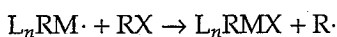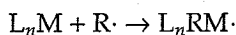
Fig. 4.25. Oxidative addition.


Fig. 4.26. Oxidative addition to Vaska's complex.

series of organic and inorganic molecules have been added to d^8-iridium and d^8-rhodium centred complexes in this manner.

The oxidative addition of alkyl halides can proceed in different ways, although the result is usually a *trans* addition independent of the mechanism [40]. In certain cases the reaction proceeds as an S_N2 reaction, as in organic chemistry. That is to say that nucleophilic attack is carried out by the electron-rich metal at the carbon atom attached to the halide, the halide being the leaving group. This process leads to inversion (Walden inversion) of the stereochemistry of the carbon atom (this can be observed only when the carbon atom is asymmetric). Note that the effect of steric hindrance in the electrophile RX on the relative rates of the reaction is the same as in organic chemistry, i.e. MeI >> EtI >> PrI >> iPrI. There are also examples in which racemization occurs. In some cases this has been explained on the basis of a radical chain mechanism. Indeed, radical scavengers have proved the presence of radicals by slowing the reaction down, and radical traps have demonstrated the expected ESR signals. The reaction sequence for the radical chain process reads as follows:

$$L_nM + R\cdot \rightarrow L_nRM\cdot$$

$$L_nRM\cdot + RX \rightarrow L_nRMX + R\cdot$$

The oxidative addition of dihydrogen to low-valent metal complexes is a common reaction in many catalytic cycles. Common electronic configuration changes involved are $d^2 \rightarrow d^0$, $d^8 \rightarrow d^6$, and $d^{10} \rightarrow d^8$. In spite of the high strength of the dihydrogen bond the reaction proceeds smoothly to afford *cis* dihydrido complexes. The bond energy of a metal–hydrogen bond is in the order of 240 ± 40 kJ mol^{-1} which is sufficient to compensate for the loss of the H–H bond (436 kJ mol^{-1}). The hydride anion is formally charged with a minus one charge and this electron count gives dihydrogen the role of an oxidizing agent!

In general, oxidative addition reactions occur at mononuclear complexes as discussed above. Oxidative addition of dihydrogen often occurs at binuclear complexes. The reaction of dicobalt octacarbonyl may illustrate this:

$$Co_2(CO)_8 + H_2 \rightarrow 2\ HCo(CO)_4$$
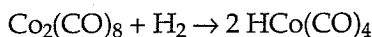
The electronic configuration of the metals change from d^7 to d^6. This reaction has also been referred to as the homolytic cleavage of dihydrogen, although no hydrogen radicals are involved in the cleavage reaction itself. In subsequent reactions this type of catalysts may indeed give rise to organic radicals. We will call it an 'oxidative addition' to a binuclear metal centre. One may have some doubt about the hydridic nature of the hydrides formed, because in the hydrido cobalt carbonyl the hydrogen atom shows an 'amphoteric' character: sometimes it reacts as an H$^-$ anion, and in other cases its reactions are best described as an H$^+$ cation (it is reported to be as acidic as sulphuric acid). Note that in the former

case the Co centre is formally monovalent, whereas in the proton case its valency is minus one. This demonstrates the ability of the metal centre to accommodate changes in effective oxidation states.

The oxidative addition of acids is another instructive example. It resembles the reactions with alkyl halides and may result in another 'amphoteric' hydride:

$$L_4Ni + H^+ \rightarrow L_4HNi^+$$
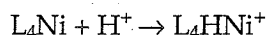
The starting material is an 18-electron nickel(0) complex which is protonated forming a divalent five-coordinate nickel(II) hydride [41]. This can react further with alkenes to give alkyl groups, but it can also react as an acid with hard bases to regenerate the nickel(0) complex. Similar oxidative addition reactions have been recorded for phenols, water, amines, carboxylic acids, mineral acids (e.g. HCN), etc.

Intermolecular oxidative additions involving C–H bond breaking is a topic which has been extensively studied recently. It is usually referred to as C–H activation; the idea is that the M–H and M–hydrocarbyl bonds formed will be much more prone to functionalization than the unreactive C–H bond [42–44]. Intramolecular oxidative additions of C–H bonds have been known for quite some time [45,46] (see Fig. 4.27). This process is termed orthometallation. It occurs frequently in metal complexes, and is not restricted to 'ortho' protons. It has considerable importance in metal-mediated synthesis.
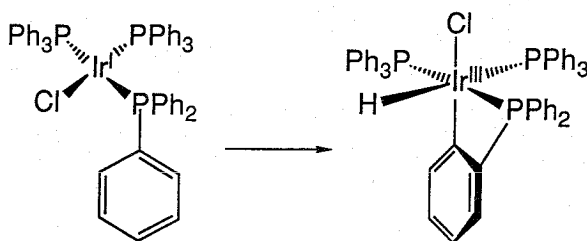
Fig. 4.27. Orthometallation.

4.3.6 Reductive Elimination

Reductive elimination is simply the reverse reaction of oxidative addition: the formal oxidation state of the metal is reduced by two (or one in a bimetallic reaction), and the total electron count of the complex is reduced by two. While oxidative addition can also be observed for main group elements, this reaction is more typical of the transition elements in particular the electronegative, noble metals. In a catalytic cycle the two reactions occur pairwise. At one stage the oxidative addition occurs, followed by, for example, insertion reactions; and then the cycle is completed by a reductive elimination of the product. Reductive

elimination can be enhanced by electron-withdrawing ligands on the metal, i.e. when the state of lower valency (electron-rich metal centre) is stabilized. Chemical oxidation (one or two electron) of a complex may also initiate reductive elimination. Only one example will be discussed here, as most reactions are directly the reverse of the ones discussed above under oxidative additions.

Reductive elimination of molecules with carbon–carbon bonds has no counterpart in oxidative addition reactions because the metal–carbon bond energies (120–240 kJ mol^{-1}) may not always be large enough to compensate for the energy of the carbon–carbon bond (370 kJ mol^{-1}), and secondly, the carbon–carbon bond is much less reactive than a carbon–hydrogen bond or a dihydrogen bond due to repulsive interactions between the attacking substituted C–C bond and the ligands surrounding the metal centre.

Examples of reductive elimination are present in the literature mostly for group 10 metals, e.g. Fig. 4.28. As outlined above, the reaction can be induced by the addition of electron-withdrawing ligands; in this case electron-poor alkenes are very effective as ligands.

In practice the reactions are less straightforward than is shown in Fig. 4.28, and several other decomposition pathways are available (see α-elimination below).

Fig. 4.28. Reductive elimination of a C–C bond.
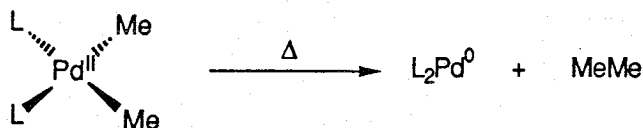
4.3.7 α-Elimination Reactions

α-Elimination reactions have been the subject of much study since the midseventies, mainly due to the pioneering work of Schrock [47,48]. The early transition metals are most prone to α-elimination, but the number of examples of the later elements is growing. A now classic example (1973!) is shown in Fig. 4.29.
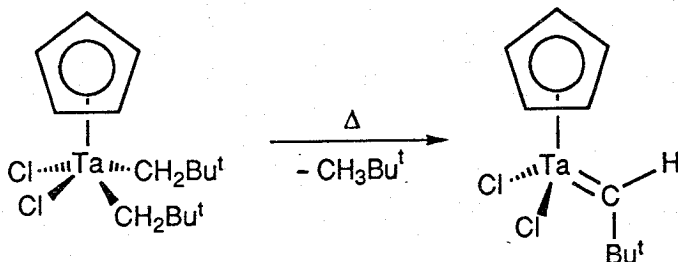

Fig. 4.29. α-Elimination.

The process is called α-elimination because a hydrogen at the alpha carbon at the metal is being eliminated (if we regard the product as a metalla-alkene the process should be called β-elimination, but this only adds to the confusion). The electron-deficient tantalum atom forms 'agostic' bonds with hydrogens in the α-positions. (Agostic interaction implies electron donation by nearby atoms or bonds to highly electrophilic metal centres which is observed spectroscopically or as a distortion in the crystal structure). In the starting material this activates one hydrogen that will then leave with the neopentyl anion as neopentane. In the alkylidene complex formed there is a strong interaction between tantalum and the electrons of the α-hydrogen of the alkylidene. Consequently, in suitable complexes α-elimination can occur twice, yielding alkylidyne complexes. See Fig. 4.30 for a simplified example with tungsten.
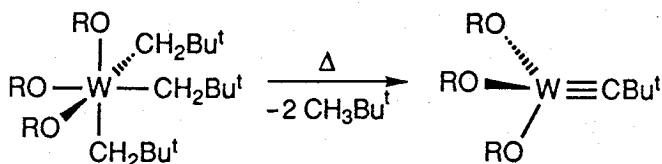
Fig. 4.30. α-Elimination giving alkylidynes.

In decomposition reactions of dimethyl–metal complexes of palladium(II) and nickel(II) one finds the formation of only traces of methane [49] which may also attributed to an α-elimination process. In regard to the valence state, note that, formally, the alkylidene ligand is considered as a neutral ligand and therefore, in the tantalum–alkylidene complex in Fig. 4.29, tantalum is trivalent. The electronic structure of the alkylidene is of course reminiscent of the corresponding oxide $CpTa(Cl)_2O$, which we would definitely call pentavalent. All that matters is that there should be a sufficient number of electrons for the multiple bonds which we draw.

4.3.8. Cyclometallation

Cyclometallation refers to a process in which unsaturated moieties form a metallacyclic compound. It is sometimes categorized under oxidative additions, but we prefer this separate listing. Examples of the process are presented in Fig. 4.31. Metal complexes which actually have displayed these reactions are $M = L_2Ni$ for reaction a, $M = Cp_2Ti$ for reactions b and c, $M = Ta$ for d, and $M = (RO)_3W$ for e. The latter examples involving metal–carbon multiple bonds, have only been observed for early transition metal complexes, the same ones mentioned under the α-elimination heading.

In examples **a** and **b** in Fig. 4.31, the metals increase their valency by two, and this is not just a formalism as the titanium(II) and the nickel(0) are indeed very electron-rich metal centres. During the reaction a flow of electrons takes place from the metal to the organic fragments which end up as anions. In these two reactions the metal provides two electrons for the process, as in oxidative addition reactions. The difference between cyclometallation and oxidative addition is that, during oxidative addition, a bond in the adding molecule is being broken, whereas in cyclometallation, fragments are added together. For reactions **c** and **d** the situation is slightly different. The formal valency of the metal increases in **c** and **d** with two units again when the alkylidene is considered as a two-electron neutral ligand. The two electrons donated by the metal in the 'oxidative addition' process were already involved in the bonding of the alkylidene, and not present at the metal centre as a surplus nonbonding lone pair (cf. square planar d^8 complexes, or the above d^2 Ti and d^{10} Ni cases). The reaction of the alkylidyne **e** is a cyclometallation reaction for which other descriptions make little sense.
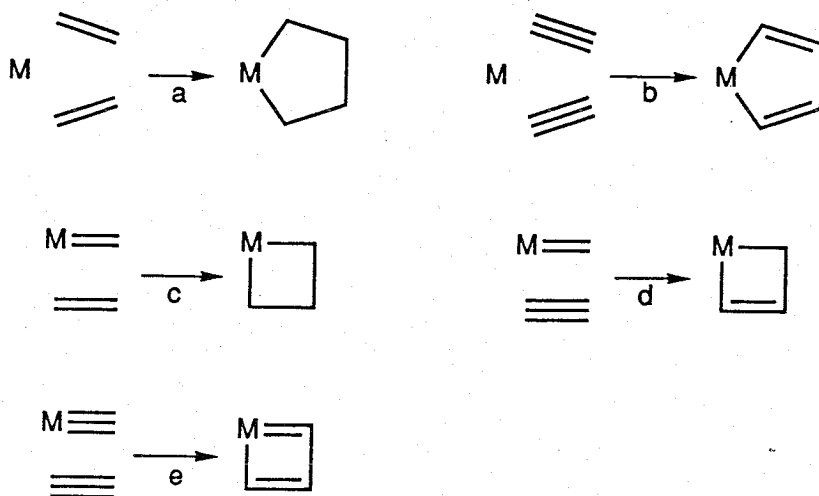
Fig. 4.31. Cyclometallations.

Three mechanisms can be proposed for the intimate reaction mechanism for c–e, analogous to the organic 2+2 cycloadditions: a pericyclic (concerted) mechanism, a diradical mechanism, and a diion mechanism. In view of the polarization of the metal(+) carbon(–) bond, an ionic intermediate may be expected. The retention of stereochemistry, if sometimes only temporary, points to a concerted mechanism.

The reverse reaction of a cyclometallation is of importance for the construction of catalytic cycles. The simple retrocyclometallations of **a** and **b** are not produc-

tive, since they would again lead to ethene and ethyne, and additional reactions have to be invoked for a productive catalytic cycle. For c–e the following retro reactions can be envisaged, leading to new products: see Fig. 4.32.
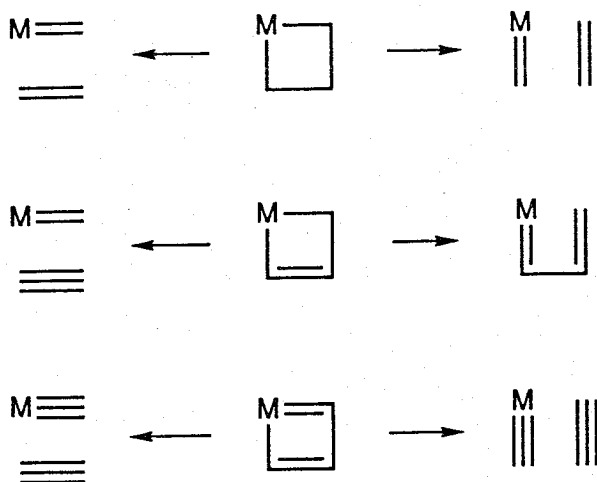
Fig. 4.32. Retro-cyclometallations.

Reaction **a** in Fig. 4.31 may be succeeded by various other reactions such as insertions, β-eliminations or regular reductive eliminations (see Fig. 4.33).
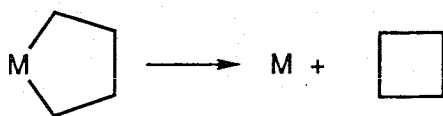
Fig. 4.33. Cyclisation through reductive elimination.

The reductive elimination reaction is governed by the common rules given in Section 4.3.6. Nickel-catalyzed cyclodimerization of butadiene [50] affords 1,5-cyclooctadiene which is used as such in a variety of chemical applications or is reduced to cyclooctene which is, *inter alia*, used for the production of cyclooctene-mers, a ring-opening metathesis product. The first step involves the coordination of a diene molecules to zerovalent nickel (and an additional ligand L). Then a cyclometallation takes place during which the nickel is transferred into divalent nickel. A reductive elimination completes the cycle regenerating nickel(0) and the two carbon–carbon bonds have been formed. Figure 4.34 shows the essential details.
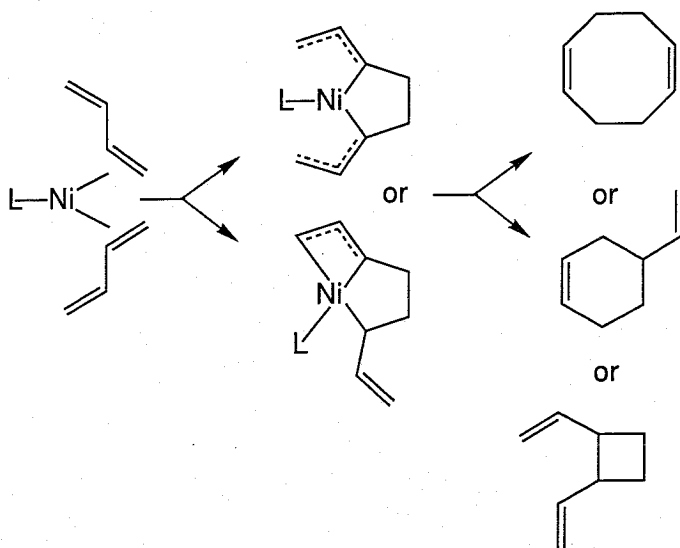
Fig. 4.34. Cyclodimerisation mechanism.

4.3.9 Activation of a Substrate toward Nucleophilic Attack

Alkenes

Coordination of an alkene to a relatively electronegative metal (it may often carry a positive charge) activates the alkene toward attack of nucleophiles. After the nucleophilic attack the alkene complex has been converted into a σ-bonded alkyl complex with the nucleophile at the β position. With respect to the alkene (in the 'organic' terminology) the alkene has undergone *trans*-addition of M and the nucleophile Nu, see Fig. 4.35. As indicated in Fig. 4.35, the overall result is the same as that of an insertion reaction, the difference being that insertion gives rise to a *cis*-addition and formation of a vacant site, and nucleophilic attack to a *trans*-addition. There is ample proof for the *trans* fashion; the organic fragment can be freed from the complex by treatment with protic acids and the organic product can be analyzed. Suitably substituted alkenes will show the *trans* or *cis* fashion of the addition. Hydrides can be added *trans* to an alkene by taking a borohydride anion as the nucleophile and adding that to a coordinated, and thus activated, alkene.

In Fig. 4.35 the nucleophile depicted is anionic, but Nu may also be a neutral nucleophile, such as an amine or H_2O. There are many alkene complexes of middle and late transition elements which undergo this type of reaction, e.g. M = Pd^{2+}, Pt^{2+}, Hg^{2+}, Zn^{2+}, $FeCp(CO)^{2+}$. The addition reaction of this type is the key step in the Wacker-type processes catalyzed by palladium.
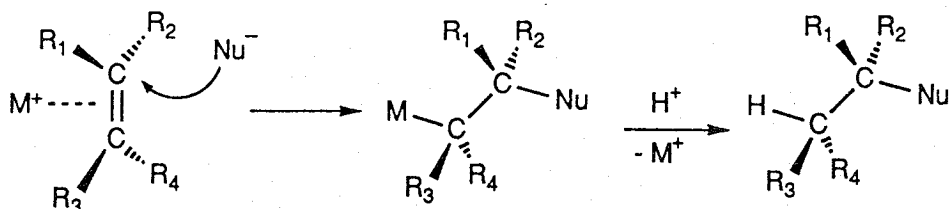
Fig. 4.35. Nucleophilic *trans*-attack on a coordinated alkene.

Alkynes

Alkynes show the same reaction, and again the product obtained is the *trans* isomer. After a suitable elimination from the metal the alkene obtained is the product of the *trans*-addition. Earlier we have seen that insertion into a metal–hydride bond and subsequent hydrogenolysis of the M–C bond will afford the *cis*-alkene product. Thus, with the borohydride methodology and the hydrogenation route, both isomers can be prepared selectively.

Carbon monoxide

Carbon monoxide, when coordinated to a metal centre, is subject to activation toward nucleophilic attack. Through σ donation and π back donation into the antibonding CO π* orbitals the carbon atom has obtained a positive character. This makes it not only more susceptible to a migrating anion at the metal centre, but also to a nucleophile attacking from outside the coordination sphere. In this instance it is more difficult to differentiate between the two pathways. There are examples showing that the electrophilicity of the carbon atom can be further increased by the action of Lewis acids complexing to the oxygen atom of the coordinated CO. Figure 4.36 shows an alkoxide attack at coordinated CO giving a carboalkoxy complex, and a borohydride attack at coordinated CO in which the boron simultaneously acts as a Lewis acid in the final product [51]. The BH_3 complexation now stabilizes the formyl complex that would otherwise be
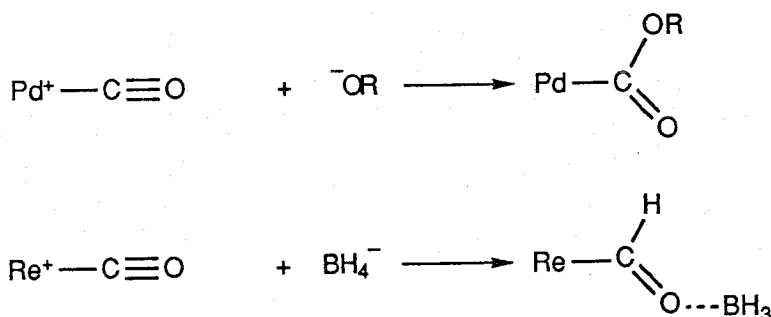
Fig. 4.36. Nucleophilic attack at coordinated CO.

$$(CO)_4Fe-C \equiv O \ + \ ^-OH \ \longrightarrow \ \left[(CO)_4Fe-C \begin{array}{c} OH \\ \diagdown \\ O \end{array} \right]^- \longrightarrow (CO)_4FeH^- + CO_2$$
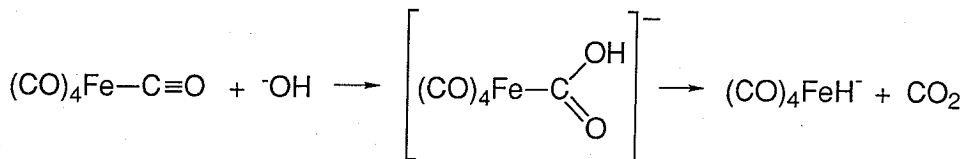
Fig. 4.37. Nucleophilic attack at $Fe(CO)_5$.

thermodynamically inaccessible. The latter reaction has so far only been of academic interest in homogeneous systems (it may be relevant to heterogeneous systems though proof is lacking). The nucleophilic attack by alkoxides, amines, and water is of great interest to homogeneous catalysis. A dominant reaction in syn-gas systems is the conversion of carbonyls with water to metal hydrides and carbon dioxide ('shift reaction'), see Fig. 4.37.

4.3.10 σ-Bond Metathesis

A reaction which is relatively new is the so-called σ-bond metathesis [52,53]. The word metathesis is used because of the now well-known metathesis of alkenes and alkynes. It is a concerted 2+2 reaction immediately followed by its retrograde reaction giving metathesis. The transition state is strongly polarized, such that in the reaction of M–R with H–H (Fig. 4.38), the transition state contains a $[H \cdots H \cdots R]^-$ M^+ unit with large negative charges at the terminal groups. The highly electronegative metal ion affords the appropriate empty orbitals for the stabilization of the complex anion in the transition state. Both late and early transition metal alkyls are prone to this reaction, but its occurrence had to be particularly invoked in the case of the early transition metals. Many similar reactions, such as the reaction of metal alkyls with other HX compounds, could be described as if they followed this pathway, but the use of the term σ-bond metathesis is restricted to those reactions in which one reacting species is a metal hydrocarbyl or metal hydride and the other reactant is a hydrocarbon or dihydrogen. Two reactions have been depicted in Fig. 4.38. There are, of course, borderline cases; when the reacting hydrocarbon is acidic, as in the case of 1-alkynes, a direct attack of the proton at
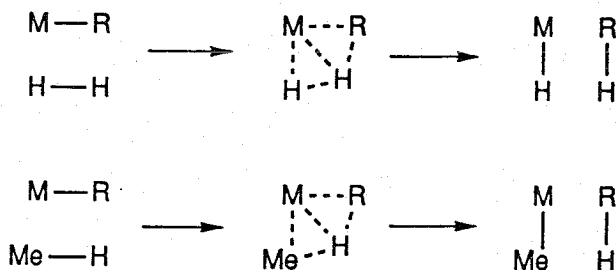
Fig. 4.38. σ-Bond metathesis.

the carbanion can be envisaged. It has been proposed that acyl metal complexes of the late transition metals may also react with dihydrogen according to a σ-bond metathesis mechanism. However, an alternative exists for the late elements in the form of an oxidative addition reaction. This alternative does not exist for d^0 complexes such as Sc(III), Ti(IV), Ta(V), W(VI), etc. and in such cases σ-bond metathesis is the most plausible mechanism. σ-Bond metathesis can also be regarded as a special case of heterolytic cleavage (see Section 4.3.11), but the latter reaction has only been observed for dihydrogen, so far, and not for alkanes.

4.3.11 Heterolytic Cleavage of Dihydrogen

Dihydrogen is said to be heterolytically cleaved when it is dissociated into a proton and a metal bonded hydride. It has been the topic of much study and discussion, and the evidence for its occurrence has been growing steadily [54,55]. In the ideal case the heterolytic splitting is catalyzed by the metal ion and a base which assists in the abstraction of the proton. In this reaction there is no formal change in the oxidation state of the metal. The mechanism has been proposed for Ru(II) complexes which can react with dihydrogen according to:

$$RuCl_2(PPh_3)_3 + H_2 \rightarrow RuHCl(PPh_3)_3 + HCl$$
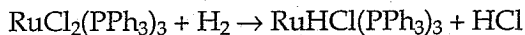
Note, however, that ruthenium has a sufficient number of d electrons to allow for oxidative addition of dihydrogen, which could then be quickly followed by reductive elimination of HCl. It is difficult to distinguish between the two pathways experimentally. Recent observations on dihydrogen complexes of ruthenium have thrown a new light on the heterolytic splitting of dihydrogen. $CpRu(L)(L')(\eta^2-H_2)^+$ reacts rapidly with NEt_3, as can be deduced from the dynamic ^1H NMR spectra, which indicate a rapid exchange of the dihydrogen complex with its conjugate base, $CpRu(L)(L')H$. This reaction is much faster than the exchange with the corresponding dihydride complex. The present studies on dihydrogen complexes may lead to a better understanding of the heterolytic splitting of dihydrogen, which is now shown to be activated towards reaction with a base through complexation to a cationic complex.

4.4 ELEMENTARY REACTION STEPS ON SURFACES

It is convenient to subdivide the reactions discussed in this section into three groups:
   (a) Reactions catalysed by metals
   In the substantial majority of cases the reaction takes place between the *adsorbed* molecule, or their fragments. This is known as the Langmuir–Hinshelwood mechanism. For very few reactions a so-called Eley–Rideal mechanism has been postulated, in which an adsorbed molecule or its fragment reacts with a molecule impinging from the gas(liquid)phase.

(b) Oxidation/reduction reactions catalysed by oxides

In many of these reactions a lattice constituent — oxygen or hydrogen — is brought into reacting molecules and the lattice defect is subsequently removed by a reaction with another reaction component, or by a reaction with another reactive centre of the same molecule. This is the so-called Mars and van Krevelen mechanism. With some oxides peroxide groups are formed on the surface (from adsorbed oxygen molecules). Radicals may form at high temperatures (1000 K).

(c) Acid base reactions catalysed by oxides

Examples are reactions initiated by the protonation, as for example carbenium ion formation from — for example — olefins (Brønsted acidic centres) or deprotonation reactions like base-catalysed aldol condensation.

4.4.1 Metal Catalysed Reactions

General features

Let us start with some features of mechanisms which are typical of metals. First, clean surfaces have a very high reactivity. Therefore, under conditions in which we usually determine the rates (or apply a reaction in practice), the surface is almost completely covered by one or another component of the reaction catalysed. For example, upon a (model) reaction $H_2 + D_2 = 2HD$, the surface of active metals is covered by a hydride like layer. Upon reaction of hydrocarbons, carbide-like species or graphitic layers can be formed. Actually, a really 'clean' reaction on metals does not exist under conditions in which one wants to measure the rate. We do not know the extent to which modifying layers retain some activity of their own. But some authors claim that these layers are very active indeed [56–59]. It has also been postulated that the firmly bound species (carbides, sulphides, graphitised carbon islands, etc.) modify the surface structure to such an extent that this change of surfaces cannot be ignored when discussing the mechanism of reactions on metals because new centres are created [60,61]. An artist's view of a working surface of a model metal catalyst (stepped single crystal surface) in contact with gas mixtures containing hydrocarbons is shown in Fig. 4.39.
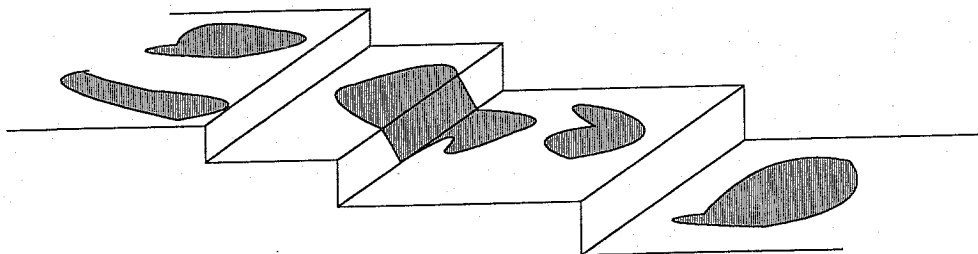

Fig. 4.39. Single crystal metal surface with cut forming steps. After adsorption of a hydrocarbon, islands are formed (preferentially on terraces) of hydrogen-lean–carbon-rich species.

A second important feature of reactions on metals is that a metal surface is a locus of very high density of active atoms. A molecule can thus be very easily bound to several contiguous atoms simultaneously or, as one says, to an ensemble of atoms [62,63]. For example, it is known that CO can be coordinated to 1, 2 or 3 (perhaps also 4) metal atoms, whereby each form shows a different frequency of CO stretching vibration $v(C \equiv O)$ (see p. 91).

All reactions on metals can be subdivided into two groups:

(i)   reactions which are not sensitive to the ensemble size variations such as (de)hydrogenations of C–C, C–O or C–N bonds; and
(ii) reactions sensitive to the ensemble size, such as hydrogenolysis of hydrocarbons (fission of a C–C bond), Fischer–Tropsch synthesis reactions (fission of the C–O bond), hydrogenolysis of C–O, C–N and most likely N–O bonds.

Also the mode of adsorption (e.g. of CO, hydrocarbons, etc.) can depend on the available ensemble size or given composition of the surface [64–68]. It appears that the heat of adsorption of various modes of CO adsorption is only marginally influenced when the required ensemble (1, 2 or 3 and more) is transferred from a pure metal into a matrix of another metal (for instance alloys with Cu, Au and Ag). When a CO molecule, monitored by IR spectroscopy, is taken as a probe of the local electronic structure of atoms (or ensembles of atoms), no pronounced effects of alloying are found 69–71].

4.4.1.1 Adsorption modes and reactivity of diatomic molecules

The adsorption of diatomic molecules on a metal surface may be considered as a competition between molecular and dissociative adsorption

$$AB_{gas} \rightarrow AB_{ads} \rightarrow A_{ads} + B_{ads} \qquad (4.4)$$
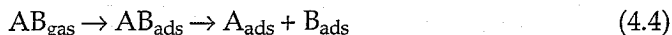
Dissociative adsorption can occur when the bonds formed between the fragments of the dissociated molecule and the surface are much stronger than the bonds within the molecule and between the molecule and the surface. For example, molecular dihydrogen, dioxygen or dinitrogen are only weakly adsorbed on the transition metals. Oxygen, hydrogen and nitrogen adatoms, on the other hand, are strongly bound on many metal surfaces. Therefore, dissociative adsorption is often thermodynamically possible, as will be discussed below.

Molecular adsorption of CO and NO is relatively strong on many metal surfaces. These adsorbates may undergo both dissociative and molecular adsorption on the same surface depending on the experimental conditions.

Figure 4.40 shows schematically three possible forms of potential energy curves for molecular and dissociative adsorption as the molecule approaches the surface. The molecularly adsorbed state can be considered as a precursor state for dissociation. The dotted curves represent molecular adsorption with a heat of adsorption
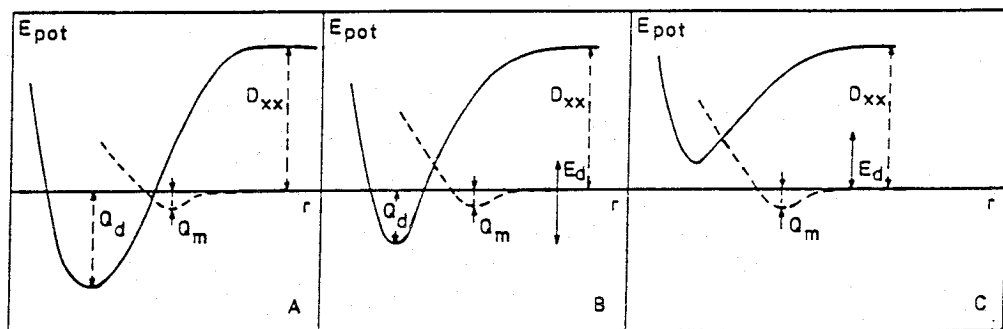
Fig. 4.40. Potential energy plots for dissociative adsorption of a molecule XX. D_{xx} is the dissociation energy of the free molecule, E_d is the activation energy for dissociative adsorption. Q_m is the heat of adsorption in the molecular state. Q_d is the heat of dissociative adsorption, and r is the reaction coordinate.

Q_m at the equilibrium distance r_m. Molecular adsorption is usually a non-activated process. The solid curves represent adsorption of the atoms following dissociation of the molecule in the gas phase, the heat of adsorption is Q_d at the equilibrium distance $r_d < r_m$, corresponding to the short-range chemical interaction.

The crossover point of the two curves determines the activation barrier of the dissociative adsorption. In Fig. 4.40A, which applies, for example, to hydrogen on transition metals, the dissociative adsorption has a zero activation energy. In Fig. 4.40B, dissociation also results in a strong chemisorption bond. However, the dissociative adsorption requires an activation energy. A typical example is hydrogen on a Cu(111) surface [72]. The activation energy for dissociation is much smaller than the dissociation energy of the free molecule. Figure 4.40C shows a typical example of an endothermic, dissociative adsorption. The potential energy of the two adsorbed atoms is higher than that of the free molecule, but lower than that of the two gaseous atoms. Therefore, dissociative adsorption can only take place when the molecule is predissociated in the gas phase and at temperatures where the adsorbed atoms are immobile on the surface. At higher temperatures, when the adsorbed atoms are sufficiently mobile over the surface, the atoms will recombine and desorb as a molecule. A typical example is hydrogen on glass or gold.

It is often observed that molecular adsorption prevails at lower temperatures and that dissociative adsorption occurs at higher temperature. This may be caused by kinetics; the activation energy for dissociative adsorption is then too high for dissociation at lower temperature. It could also have a thermodynamic reason. If the number of surface sites where adsorption can take place is equal for molecular and dissociative adsorption, the surface can accommodate twice as many molecules in the molecular state than in the dissociative state. Hence, molecular adsorption will prevail if the heat of dissociative adsorption is not very much higher than the heat of molecular adsorption. The entropy change upon
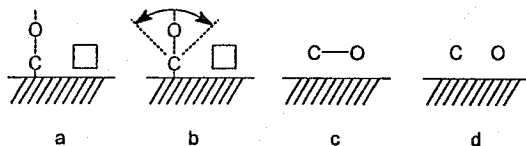
Fig. 4.41. Molecules like CO are bonded in most of the group 8–10 metal surfaces with the molecular axis perpendicular to the surface (a) or slightly tilted. The amplitude of vibration around the surface normal increases with increasing temperature (b). At a certain temperature an oxygen–metal bond is formed (c) and dissociation occurs (d).

adsorption is negative and, consequently, desorption will occur at a sufficiently high temperature. In the case considered above only half the number of molecules can be adsorbed in the dissociative state compared to the molecular state. As a result the entropy of the system will be lower for molecular adsorption and dissociation can occur at higher temperatures.

Dissociative adsorption requires a cluster of several free and contiguous metal atoms in an ensemble on the surface. Therefore it is often found that dissociation occurs only when the surface coverage is low and that molecular adsorption takes place above a certain coverage.

A diatomic molecule has to be adsorbed parallel to the surface in order to dissociate. The more favourable adsorption complex for molecules like CO on a group 8–10 metal surface is that in which the molecular axis stands perpendicular to the surface. It has been demonstrated by ESDIAD (electron stimulated desorption, ion angular dependence) that the molecular axis vibrates with regard to the surface normal and that the amplitude of vibration increases with increasing temperature; this is shown in Fig. 4.41.

At the dissociation temperature the vibration amplitude has become sufficiently large that a bond between the O atom and the metal surface can be formed resulting in dissociation.

Before we present a survey on the adsorption of several simple gases some general aspects of the dissociative adsorption will be treated. Table 4.1 tabulates the dissociation energies of reactants in the gas phase. Table 4.2 shows some examples of the heats of formation of hydrides, nitrides, carbides and oxides.

The following relevant conclusions emerge:

(1) Dissociation in the gas phase becomes more difficult in the order $H_2 < O_2 <$ NO < CO and N_2.

(2) The order in strength of the metal–X bond (X = H,C,N and O) is M–H < M–C < M–N < M–O for the same metal.

(3) From (1) and (2) it follows that dissociative adsorption on a certain metal surface become more favourable in the order N_2, and CO < NO < O_2.

(4) For the transition metals the M–X bond strength increases for metals further to the left in the periodic table and it decreases on going down from $3d$ to $5d$ metals.

TABLE 4.1

Dissociation energies in the gas phase

d^0_{298}	kJ mole^{-1}
H_2	436
O_2	498
NO	631
N_2	945
CO	1076

TABLE 4.2

Heats of formation of Ti, Mo, Pd and Ni hydrides, carbides, nitrites and oxides at 198 K, 1 bar. Values in kJ mole^{-1} of H, C, N, or O

Ti		Ni	
TiH$_{1.7}$	− 69*		
TIC	−226	Ni$_3$C	+ 46
TiN	−336	Ni$_3$N	+ 1
TiO$_2$	−456	NiO	−244
Mo		Pd	
Mo$_2$C	− 23		
Mo$_2$N	− 69		
MoO$_2$	−272	PdO	− 85

(All values are taken from Ref. [73], except * (from Ref. [74].)

The surface structure may have an additional influence on the dissociation. In general, close-packed surfaces are the least active and rough surfaces or surfaces with steps or kinks the most active in dissociation.

4.4.1.2 Elementary theory of dissociation and association reactions on metal surfaces

Let us now analyse dissociation and recombination in detail. As we saw in the previous sections dissociative adsorption is a process consisting of at least two consecutive elementary steps. Molecular adsorption precedes dissociation. Dissociation occurs when reaction (4.4) is thermodynamically feasible. We learned in Section 4.2.1 that the surface adatom bond energy varies more than the molecular adsorption bond with variation of metal. Adsorption of atoms is favoured by metals with a partially filled d valence electron band or metals of a low work function. CO will dissociate on the first row transition metals (except
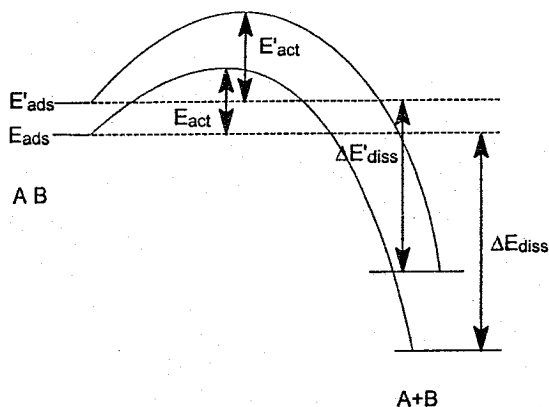
Fig. 4.42. Relation between δE_{act} and δE_{diss} (schematic).

on Cu), it will barely dissociate on Rh, and not at all on Pt or Ir. O_2 will dissociate on all transition metals, including Cu and Ag, but not on Au.

According to the Brønsted–Polanyi relation, the change in the activation energy relates to the differences in overall reaction energies:

$$\delta E_{act} \approx \frac{1}{2} \delta \Delta E_{diss} \tag{4.5a}$$

with

$$\delta E_{act} = E'_{act} - E_{act} \tag{4.5b}$$

and

$$\delta \Delta E_{dis} = \Delta E_{dis} - \Delta E'_{dis} \tag{4.5c}$$

E and E' refer to energies on two surfaces of different reactivities. The relation is sketched for the surface-dissociation in Fig. 4.42.

On a transition metal surface the dissociating molecule prefers a specific reaction-path [75]. This is sketched in Fig. 4.43 for CO on a (111) surface . The surface atoms generated by dissociation prefer high coordination sites. According to the nomenclature of organometallic chemistry such sites are denoted μ_n sites, n being the number of metal atoms involved in the chemisorptive bond. CO bonded with one molecular atom to the surface is η^1 bonded. Side-on adsorbed CO is η^2 bonded. When the atoms are adsorbed in neighbouring adsorption sites (e.g. a and b, Fig. 4.43) they experience a large repulsive interaction. The effective number of neighbours of the surface metal atom has increased by adsorption, which reduces the bond strength of the atoms that are coordinated to this surface-metal atom. When one of the atoms adsorbs in site a, the other metal surface sites, c or d, are positions where the dissociated atoms share the least number of surface atoms and hence have the smallest repulsive interaction.

The activation energy is least when the CO bond is weakened because of its interaction with the metal surface. Electron transfer from the metal surface into antibonding molecular orbitals weakens the CO bond. This is a very general

a. initial non-dissociated state

b. transition state

c. final dissociated state
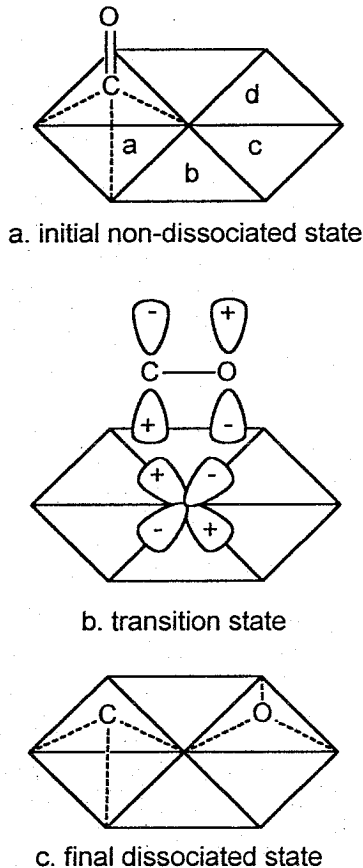
Fig. 4.43. Dissociation of CO (schematic).

feature of dissociative adsorption. The dissociation energy of adsorbed molecules decreases when they are adsorbed with considerable electron transfer from the metal surface to the adsorbate.

For instance, O_2 molecules readily dissociate on the Ag (110) surface. The molecule is adsorbed as O_2^-, with a charge of the order of ~−1.6 a.u. [76,77]. Chemisorbed CO undergoes considerable CO bond weakening, because electron donation to CO populates its antibonding $2\pi^*$ orbitals (see Fig. 4.4). The antibonding bond (i.e. weakening orbitals) are usually antisymmetric with respect to a molecule or bond symmetry axis. The dissociating molecule, parallel to the surface, has to interact with surface orbital fragments of proper symmetry in order that electron donation may occur. As sketched in Fig. 4.43 d_{xz} or d_{yz} orbitals have the proper symmetry. So, for a low dissociation energy barrier, interaction with occupied d surface atomic orbitals asymmetric with respect to the surface is essential. Whereas, for a dissociation reaction, electron transfer between surface

a

b

Fig. 4.44. Formyl formation on a palladium surface (schematic). (a) Molecule fragment rearrangement on the metal surface. (b) σ-Orbital interaction scheme.

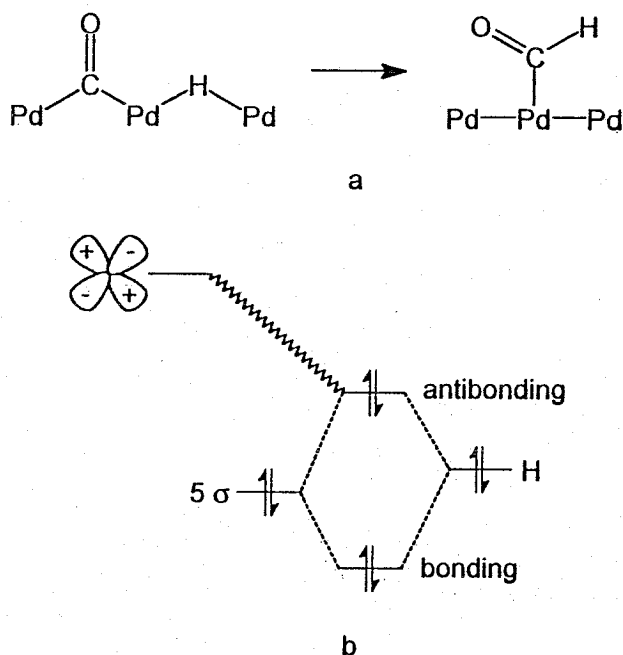and adsorbate is favourable, the reverse is the case for the association reaction. This is obvious for diatomic molecules, but it is also valid for more complex reactions. We will analyze this for the formation of a formyl intermediate from adsorbed H and CO. For CO and H chemisorbed to Pd this reaction is sketched in Fig. 4.44.

When the hydrogen atom and CO move together, a repulsive interaction between the doubly occupied CO 5σ orbital and the H s orbital develops [78–80]. This is sketched in Fig. 4.44. A bonding and an antibonding orbital fragment are formed. Both orbitals are doubly occupied, hence they interact repulsively. The repulsive interaction is relieved when electrons from the antibonding orbital can be back-donated to the metal. An empty d_{xz} and d_{yz} orbital has a proper symmetry for that. Therefore formyl formation is expected to occur on metal surfaces with empty, low-lying d valence orbitals. All transition metals, except Cu, Ag and Au, have empty d orbitals. Metals with a high work function, such as Pt and Pd, are particularly suitable. The competitive reaction of CO dissociation will be suppressed on such metals. The formyl formation mechanism described here for a metal surface was first discovered in a theoretical study of a Pd^{2+} organometallic complex [81]. Pd has to be an ion because Pd atoms have no empty d atomic orbitals.

Formyl intermediates are easily hydrogenated to give methanol. Copper based catalysts are very active methanol catalysts. Because Cu has a completely filled d
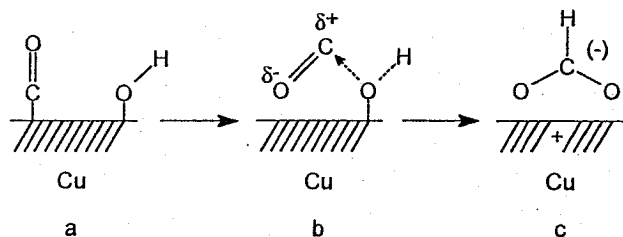
Fig. 4.45. Formate formation from CO and Cu (schematic).

valence electron band, methanol formation cannot proceed on metallic Cu via formyl formation. On a Cu catalyst methanol formation can occur via the formate intermediate, which is subsequently hydrogenated to methanol. Formate formation probably occurs by reaction of a surface hydroxyl with chemisorbed CO. Because of the weak interaction between Cu, Cu^+ and CO and the charge build-up on the CO oxygen atom, an intermediate, as sketched in Fig. 4.45, is most likely. Methanol formation on Cu occurs most readily by hydrogenation of CO_2. Intermediates like 4.43b and c can now form readily. Below we will discuss a related surface intermediate formed in the Cu-catalysed oxidation of CO.

Another important association reaction is hydrocarbon formation by carbon–carbon bond closure. This occurs with hydrocarbon fragments in the presence of hydrogen or from carbon monoxide (Fischer–Tropsch process). The surface reaction

$$+ CH_4 \tag{4.6}$$

readily proceeds on the transition metals with d valence electron vacancies, but is prohibited on metals with excessively strong M–C or M–H bonds [82,83]. The rate of recombination is expected to be a maximum on Pt, a metal with the weakest M–C bond. Recombination of methyl radicals appears to be prohibited because of repulsive interactions between the methyl hydrogen atoms when the methyl groups approach each other. Steric repulsion decreases when the surface hydrocarbon fragments become less saturated with hydrogen. The interaction of a CH_2 and CH fragment is sketched in Fig. 4.46.

Now a close approach is possible, and interaction of several orbitals can also occur. Besides the repulsive interaction between surface σ bonds, a stabilizing interaction between fragment p orbitals also takes place. This results in a relatively low activation energy of recombination that only weakly depends on the metal–carbon bond strength. Competition between C–C chain growth and methanation or termination (CH formation) favours C–C chain growth as the metal–carbon bond energy increases.
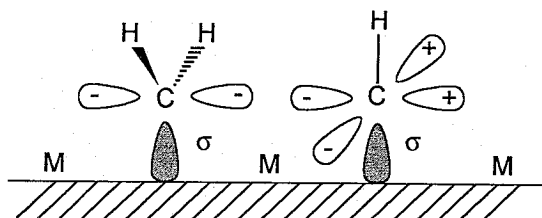
Fig.4.46. Recombination of CH_2 and CH species.
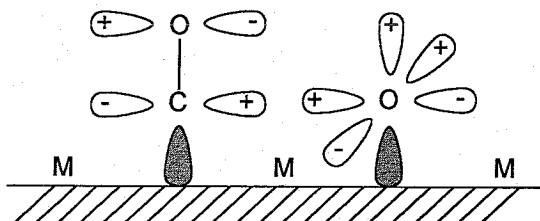
Fig. 4.47. The oxidation of CO by O (schematic).
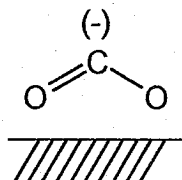
Fig. 4.48.

The p orbital stabilizing interaction appears to be quite common. It also lowers the activation energy for the O and CO recombination reaction to form linear CO_2. On a surface that interacts strongly with CO, e.g. a transition metal with partially filled d valence electron orbitals, the reaction proceeds as sketched in Fig. 4.47.

On a low work function metal or one with a filled d valence electron band the bended CO_2 (Fig. 4.48) becomes stabilized and reaction occurs analogously to the CO–OH recombination reaction.

As already indicated in the discussion on formyl formation, the transition state on a metal surface may be closely related to that found in the organometallic complexes used in homogeneous catalysis. The p orbital stabilizing interactions have also been shown to play an important role in insertion reactions occurring in organic-metallic complexes [84,85]. It explains, for instance, the higher activa-
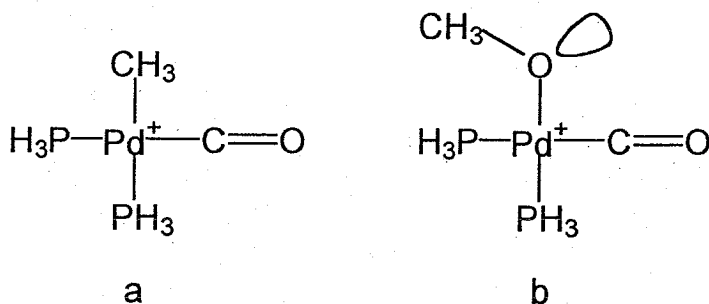
Fig. 4.49. The lone-pair orbital of the methoxy group has a stabilizing interaction with the CO $2\pi^*$ interaction. This interaction is absent with the methyl fragment.

tion energy for insertion of CO in a methyl group compared with a methoxy group in Pd complexes, sketched in Fig. 4.49.

Since dissociation of a molecule requires a certain minimum ensemble of surface atoms, the reactivity of very small metal clusters tends to increase with particle size. Once a cluster with the proper ensemble of atoms has become available the reactivity decreases, because the ensemble acquires an increasing number of metal atom neighbours. These two basic features, illustrated in Fig. 4.50, may explain the frequently observed maximum in cluster reactivity as a function of the number of metal atoms.
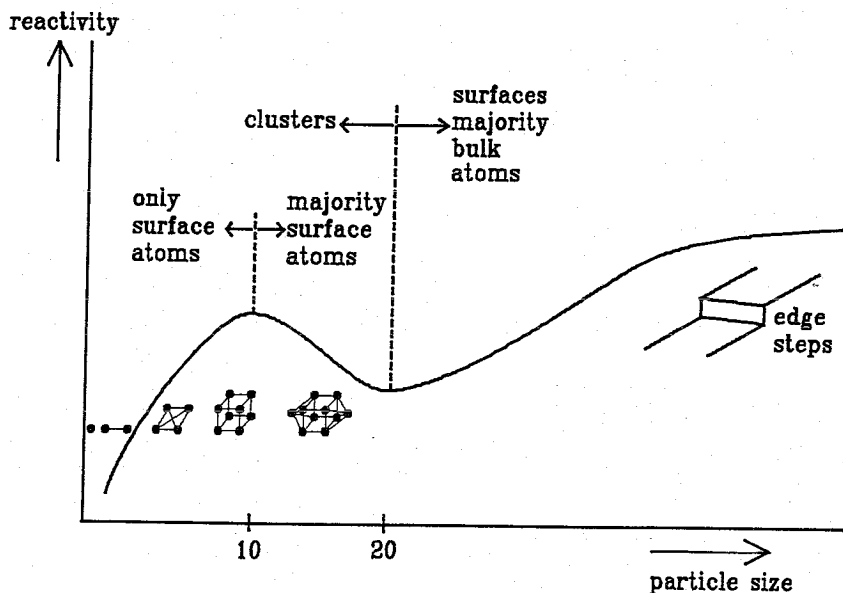
Fig. 4.50. The rate of adsorption as a function of particle size (schematic).

4.4.1.3 CO adsorption

In order to understand the catalytic properties of the various group 8–10 metal surfaces the interactions among neighbouring adsorbed species and their effects on the surface processes should be known, since the surfaces may be covered with different kinds of adsorbates during the reaction. An interesting example is provided by O_2 and CO coadsorption on the Pd (111) surface. Some of the relevant results are summarized here.

Oxygen adsorption is inhibited by pre-adsorbed CO. At coverages below θ_{CO} = ⅓, O_{ads} and CO_{ads} form separate domains on the surface. Remarkably, the behaviour is different when O is pre-adsorbed. Then formation of mixed phase of O_{ads} and CO_{ads} occurs (with local coverages of $\theta_O = \theta_{CO} = 0.5$) which are embedded into CO domains. When these mixed phases are present CO_2 is produced even below room temperature. Co-adsorption studies on other noble metal surfaces are consistent with this picture: pre-adsorbed CO inhibits the dissociative adsorption of oxygen whereas CO does adsorb on a surface covered with O. The CO-covered surface is densely packed with CO, but the oxygen atom-covered surface is less densely packed with CO.

The interaction of co-adsorbed H and CO has been studied on a variety of single crystal and polycrystalline surfaces under conditions where reaction does not occur [86]. The following phenomena have been observed: displacement of adsorbed H by CO, blocking of H adsorption by pre-adsorbed CO, segregation of the co-adsorbed species, formation of mixed layers, decreases in the H desorption temperature, but also enhancement in the uptake of CO by the presence of pre-adsorbed H, and formation of new desorption peaks in the TDS. There is no evidence for the formation of directly bonded H–CO from 'on-top' sites into bridged sites.

In conclusion, the main effects found for coadsorption are blocking, island formation, displacement by the component with higher heat of adsorption and site conversion. Attractive interactions may occur between the two adsorbates. Hence, the catalytic reactions can be discussed on the basis of the adsorption of the individual reactants in combination with the coadsorption effects mentioned above.

4.4.1.4 Surface reactions of small diatomic and triatomic molecules

The crystal face dependence and the activity of the various group 8–10 metals can be understood in terms of the metal–oxygen bond strength. On an active metal both O_2 and H_2 are dissociatively adsorbed, oxides are not formed under reaction conditions, and the heat of adsorption for O_{ads} is relatively low.

Usually, temperatures of 300–600 K are required for the oxidation of CO over the active metal catalysts Pt, Pd, Ir, Rh, Ru and Ni. It has been established that the

dominant mechanism of the reaction is the Langmuir–Hinshelwood (LH) mechanism:

$$CO \rightleftarrows CO_{ads}, \qquad O_2 \rightarrow 2\,O_{ads}, \qquad O_{ads} + CO_{ads} \rightarrow CO_2$$
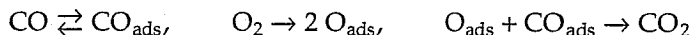
The activation energy is lower over Pt than over Ir, Rh, Pd and Ru catalysts [87]. CO adsorption inhibits dissociation of O_2 at low temperatures. Because of CO desorption, inhibition becomes less with increased temperatures. The overall rate of oxidation decreases at higher temperatures because of the decrease in surface coverage.

Figure 4.51 shows the rate of CO_2 production over the (111), (100), (410) and (210) surfaces of a Pt-0.25–Rh-0.75 single crystal as a function of temperature using a 2:1 mixture of CO and O_2 for a total pressure of $2{\times}10^{-7}$ mbar [88]. It shows that the reaction rate increases rapidly between, 400 and 500 K up to a temperature T_m where a maximum is reached, after which it slowly decreases with increasing temperature. The temperature at which the maximum occurs increases with increasing the strength of the CO interaction. Similar behaviour has been found on a large number of Pt, Pd, Ir, Rh and Ru surfaces.

In Fig. 4.52 the activity of H_2 oxidation for different metals is plotted as a function of heat of oxygen adsorption. A volcano-type plot is formed. A maximum in rate is found for the metal that can dissociate O_2, but does not bind CO or oxygen too strongly. Gold cannot dissociate O_2, tungsten is inactive because it
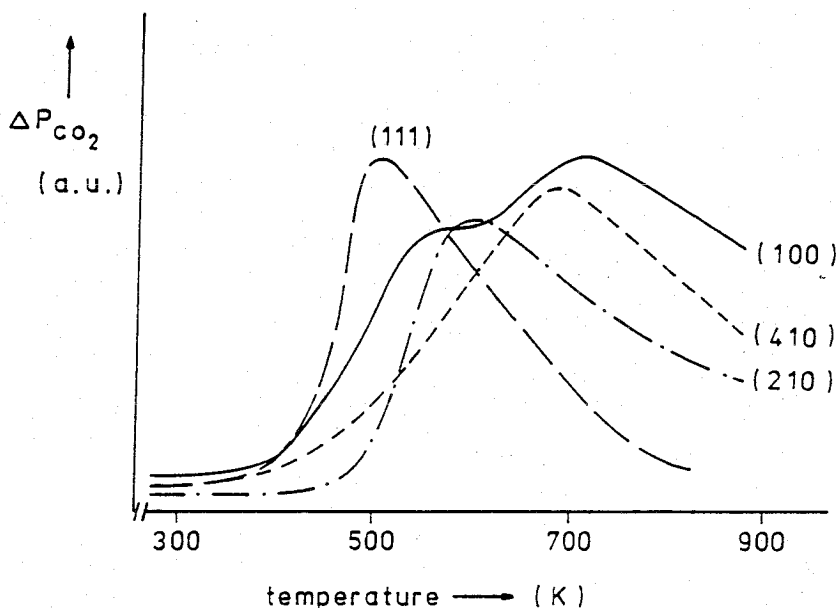

Fig. 4.51. Steady-state rates of CO_2 production for the CO + O_2 reaction over the (111), (100), (410) and (210) surface of a Pt-0.25–Rh-0.75 single crystal (from ref. 88).
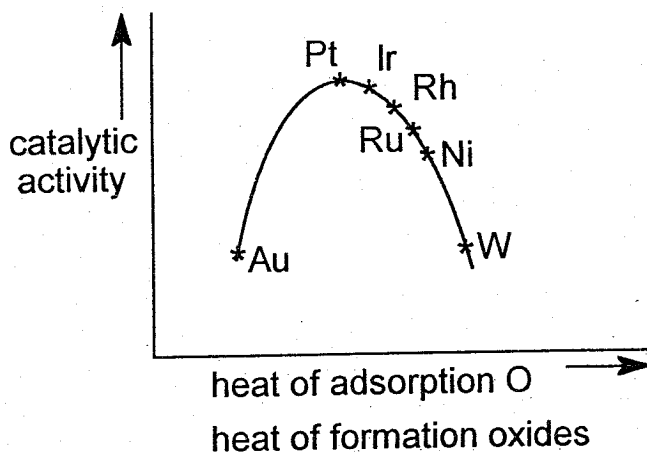
Fig. 4.52. Volcano plot for carbon monoxide oxidation.

forms a stable surface oxide layer. Vulcano plots as shown in Fig. 4.52 illustrate the Sabatier principle, stating that optimum activity is obtained when catalysts neither binds intermediates too strongly so as to inhibit adsorption to the surface, nor interacts too weakly so as to cause no initiation of the reaction.

Dissociation is often a crucial step in a catalytic reaction chain. However this is not always the case. Metals active for the $O_2 + H_2$ reaction are the noble metals of group 8–10, especially Pt, a metal with a low O–metal bond strength. The same metals are active for the $CO + O_2$ reaction. The most active metals do not easily break the C–O bond and do not form oxides under reaction conditions. Both reactions are Langmuir–Hinshelwood reactions between adsorbed O and adsorbed H or CO. Desorption of products of the reaction intermediates here is reaction rate controlling.

Active catalysts for the NO + CO reaction must be more active in bond breaking: NO must dissociate, whereas the C–O bond must stay intact. Dissociation is followed by a Langmuir–Hinshelwood reaction of O with adsorbed CO.

For the methanation and NH_3 synthesis reaction the metals must be still more active in bond breaking: the CO and N_2 molecule both must dissociate under reaction conditions and the reaction then proceeds by hydrogenation of C, N and O on the surface. Additional factors that determine the performance of the metal in these reactions are the nature and bond strength of C, N and O on the surface.

4.4.1.5 Adsorption modes and reactivity of hydrocarbons

Hydrocarbons form a variety of species on metal surfaces (shown in Fig. 4.53), which Burwell [89,90] once called "The organometallic zoo" of surface com-
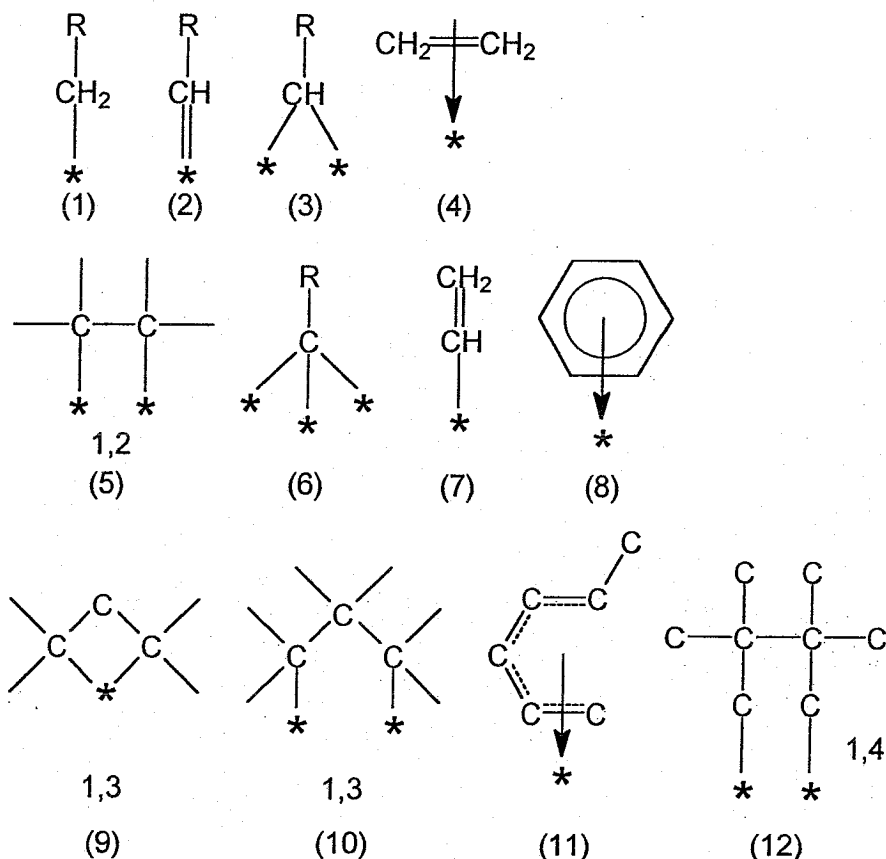
Fig. 4.53. Various organometallic species formed on metal surfaces (only well documented ones are shown — see text).

plexes. Passing over the individual species, we shall discuss what we know about their reactivity in relevant hydrocarbon reactions.

The species (2) or (3), and those from (5) to (7) (all in Fig. 4.53) are supported by both chemical and spectroscopic arguments. It is important to note [91–93] that there are important 'chemical' arguments (exchange reactions) for the presence of multiply-bound species in the presence of hydrogen (or D$_2$), since the presence of H$_2$ suppresses the formation of the multiply bound species so much that they are no longer detected at the temperatures at which vibration spectra are monitored [94]. Species (4) and (5) can be considered as alternatives, both originating from the adsorption of ethene on transition metals. Species (4) is preferred on Pd, (5) on Pt [95]. Labelled (C*) isohexanes have been used [96] to show that two mechanisms are operating when, for example, 2-methylpentane is converted into 3-methylpentane [96] (transition state structures are in brackets).
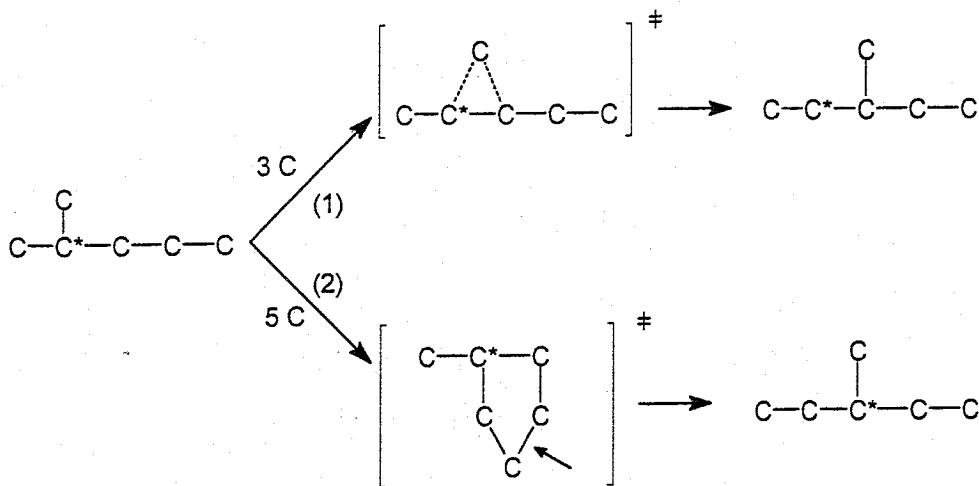
Scheme 4.1.

The required intermediates comprise either 3C atoms (route 1) or 5C atoms (route 2). Isomerisation, as upon (2), is only possible when a *cyclic* intermediate species is formed, such as on the right side of the scheme, which species opens the ring at the place indicated by an arrow. The 3C-cyclic intermediate has to have a form like species (9) or (10) of Fig. 4.53 (possibly with some carbons bound multiply to the metal surface), and with the 5C cyclic intermediate the best indications exist for an intermediate (5).

Intermediates can be converted from one to another. For example, the π-complexed ethene can be converted into ethylidyne species (6) on a hydrogen-lean surface of Pd (100) [97–99].

The reactivity of various species in Fig. 4.53 differs quite a lot. Judging on the grounds of the now available deuterium exchange reaction data, one can say that the singly bound (1) and π-complexed species (4) of Fig. 4.53 are the most reactive forms [99–105], while the multiply-bound species, in particular those like (6), are rather unreactive.

Surface complexes originating from hydrocarbons are those on which the information in the literature is most complete. Oxygen containing molecules have been also studied by the spectroscopic and chemical methods quite intensively.

Figure 4.54 shows schematically the species observed upon adsorption of alcohols (alkoxy species), aldehydes, ketones and carboxylic acids. When alcohols are adsorbed, the methoxy group is always formed very easily with all metals (the evidence for it is from D_2 exchange reactions [106,107] and various spectroscopic techniques: for the latter see the references below). However, only on Cu and Ag does the stability of this intermediate allow a comfortable study. With the transition metals, the dehydrogenation proceeds very quickly and the
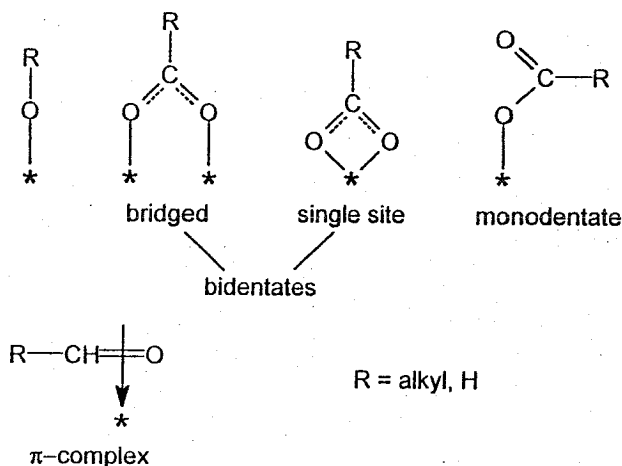
Fig. 4.54. Various surface complexes formed upon adsorption of alcohols, aldehydes or acids, on metals and oxides.

authors of Refs. 108–119 collected evidence that the dehydrogenation passes the following stages: molecular methanol → methoxy → formaldehyde → formyl → CO. The reverse order would convert syngas into methanol. Formaldehyde, and probably with it other higher aldehydes and ketones too, is adsorbed by a weak π-complex-like side-on-bonded (shown) or an 'end-on-bonded' (the most likely one) [111–115]. The rapid dehydrogenation of methoxy species can be slowed down by modification of the transition metal surfaces by — for example — sulphur deposition or by surface carbide formation. The sites next to the adsorbed methoxy species became occupied, hence preventing activation of the CH bonds.

4.4.2 Mechanism of the Reactions on Oxides

4.4.2.1 Reactions related to the oxygen transfer

It is convenient to subdivide the low temperature and medium range temperature oxidation reactions according to the character of the oxygen active species;

(1)   electrophilic oxidations, with species O_2 or O;
(2)   nucleophilic oxidations with a species O (lattice oxygen).

This is related to the temperature range (see Scheme 4.2 [116]) and the type of the catalyst. Type (1) reactions prevail (but are not exclusive to) with 'early' transition metal oxides, strongly basic oxides like MgO and rare earth oxides; type (2) reactions prevail on the oxides of the 'late transition metals' (group 6 and higher) and on Cu oxides.

R· O· O_2·

reactions of free (desorbing) radicals,
combined with surface reactions

$T, °C$

600 —

O^{2-}

Mars and Van Krevelen mechanism

200 —

O· O_2·

reactions of adsorbed radicals

Scheme 4.2.

oxygen
containing
molecule

oxygen free
molecule
(reductant)

M☐MOMOMO
OMOMOMOM

MOMOMOMO
OMOMOMOM

$1/2\ O_2$

oxygen
containing
molecule

a molecule
with an
oxygen atom
removed
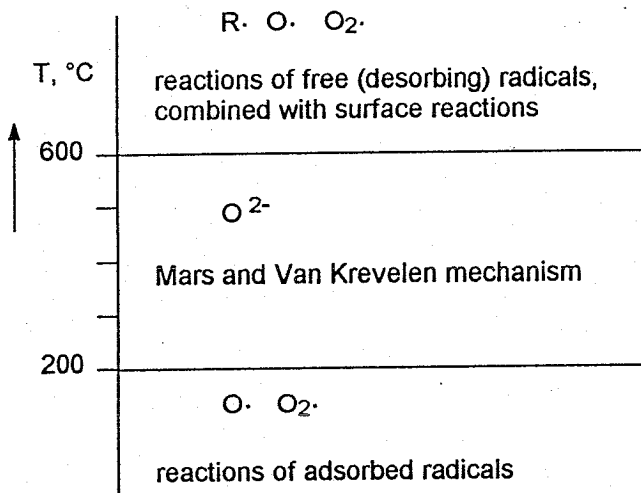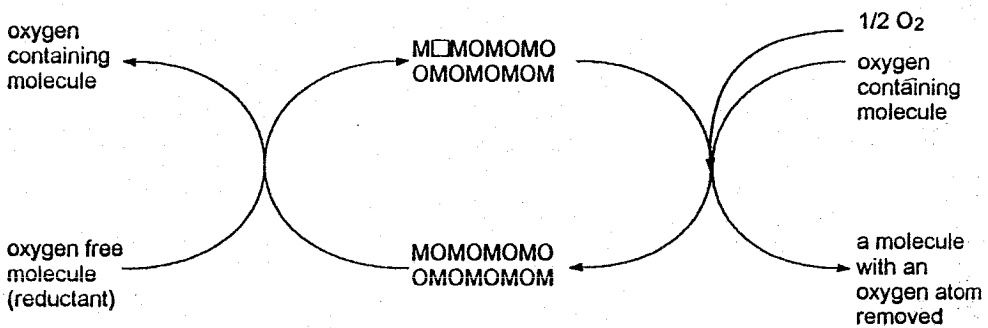
Fig. 4.55. Mars and van Krevelen redox mechanism of the selective oxidation (left side) or selective reduction (right side). Both reactions can also be coupled into a system of two selective reactions running simultaneously.

The type (2) reactions are frequently of a very high selectivity, which is widely exploited by industry (about 20% of all chemicals are produced by oxidation reactions). The type (2) reactions proceed by the so called Mars and Van Krevelen mechanism [117], which is schematically shown for an oxidation reaction in Fig. 4.55.

Two remarks have to be made here. First, the reader should realize that with reactions on metals, the largely prevailing mechanism (perhaps reactions on hydrides or carbides could be the rare exception) is that of Langmuir–Hinshelwood, with a surface reaction among the *adsorbed* species and with rates propor-

tional to the surface coverages θ_s. Upon a reaction running by the Mars and Van Krevelen mechanism, a *lattice component* of the catalyst appears in the product molecules! Second, upon oxidation, lattice oxygen appears in the product and the vacancy is replenished by a dissociative adsorption of dioxygen, which mechanism can be reversed and used for a selective reduction (selective removal of one single oxygen atom) of organic molecules. Then the vacancy is created by a common reductant (CH_4, H_2) and replenished by oxygen from the organic molecule. In this way, nitrobenzene can be selectively reduced to nitrosobenzene (without undesired reduction to aniline), and aromatic acids (or esters) can be converted into corresponding aldehydes (etc.). It might be practically interesting to combine two selective steps, for example, a selective reduction of nitrobenzene and a selective oxidative dehydrogenation of — say — ethylbenzene [118]. Oxides or mixed oxides can also be used to an advantage for hydrogenation, hydrogenolysis or dehydrogenation (oxidative, or in the absence of oxygen) reactions. Hereby, the heterolytic splitting of the H–H or C–H bonds usually plays the crucial role [119,120]. Limiting the CH dissociation suppresses hydrogenolysis.

Oxides are more complicated systems than metals. However, with oxides, too, some information on the molecular level mechanism is available. For example, it has been established that variously coordinated active metal ions posses a different activity [121]. For selective oxidation and reduction, the octahedral oxygen is frequently more reactive than the tetrahedral one. The oxidation reactions are also known to be crystal face sensitive or even specific [122–124].

Oxidation reactions (and the reversed reactions of the selective removal of oxygen, too) are practically very important. In the past, attention was mainly concentrated on oxidation of olefins, but nowadays research is focused on saturated hydrocarbon molecules. Some important reactions are listed in Table 4.3.

Silver is an important metallic catalyst for the selective oxidation of ethylene. The silver catalyst is used to selectively convert ethylene to ethylene epoxide, an important intermediate for antifreeze. Whereas the epoxidation of ethylene proceeds with high selectivity on oxidic silver phases, metallic silver surfaces give only total oxidation of ethylene. Relatively electron-deficient O is created on oxidized silver surfaces and this readily adds to the electron-rich ethylene bond.

A huge volume of information has been collected on the selective oxidation of olefins, with propene as a typical and most frequently studied molecule. First, it has been established that the reaction is induced by a dissociative adsorption, which — with propene — leads to allyl species [119,120] CH_2–CH–CH_2. These species are subsequently converted by oxygen of the oxide lattice into the oxygenated product (acroleine, with propene). The frequently used catalysts are combinations of two oxides, like, for example, $Bi_2O_3MoO_3$. In some cases it appeared to be possible to identify the various functions of individual active sites on the

TABLE 4.3

Examples of commercialized selective oxidation reactions of organic molecules

Feed	Product
ethylene	ethylene oxide
	acetaldehyde (liquid phase)
propylene	acrylonitrile (ammoxidation)
	propylene oxide (in liquid phase)
	acrylic acid
isobutene	methyl methacrylate
n-butane	maleic anhydride
naphthalene	anthraquinone
methanol	formaldehyde

catalysts. For example, Bi sites are known to be mainly responsible for the allyl formation, while the metal–oxygen bond strength is made more suitable for the extraction–addition of oxygen by the formation of mixed Mo–O–Bi bonds. When the feed consists of propene, oxygen and ammonia, acrylonitrile is produced, an important monomer for the production of polymers.

Recently, attention has been shifted to the oxidative functionalisation of saturated molecules. Reactions such as from ethane $\rightarrow$ vinylchloride, propylene $\rightarrow$ methacrylic acid, or butane $\rightarrow$ maleic anhydride, became a target of many research efforts. A catalyst which appeared to be very versatile in such reactions is vanadyl pyrophosphate, $(VO)_2P_2O_7$. The mechanism of oxidative functionalisation is not yet known in all details, but there are many indications that it is in some crucial steps different from the mechanism operating with olefins.

4.4.3 Catalysis by Solid Acids

4.4.3.1 General introduction

Oxidic surfaces in particular develop acid or basic properties which are important in catalysis. We will approach this subject first by taking as a starting point the ionic bond model [125]. The lattice is considered to consist of cations and anions held together by electrostatic interactions. Later we will discuss a more balanced theory that also accounts for covalent bonding aspects.

Surface Lewis acidic or basic sites are created on ionic surfaces because surface atoms have a lower coordination number compared to their bulk values. A condition for surface stability is that the sum of the charges over the surface unit

cell is zero and the surface is overall neutral. A useful method to estimate the degree of coordinative unsaturation on an ionic surface is to use Pauling valencies and to compute charge excesses. The Pauling valency, v, is defined as:

$$v = Q/C \tag{4.7}$$

Where Q is the formal ion charge and C its coordination number.

For the Mg^{2+} ion, the Pauling valency equals

$$v^+ = \frac{2}{6} = \frac{1}{3} \tag{4.8a}$$

and for the O^{2-} ion, the valency becomes

$$v^- = -\frac{2}{6} = -\frac{1}{3} \tag{4.8b}$$
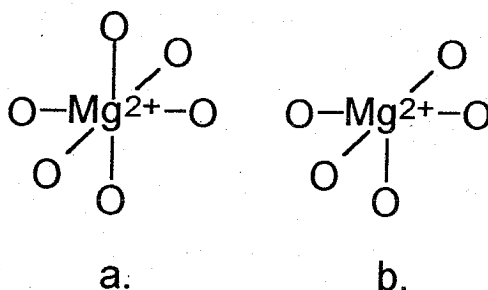
Fig. 4.56. (a) Six-coordinated Mg^{2+} of bulk oxide. (b) Five-coordinated Mg^{2+} on the MgO(100) surface.

On the surface the charge excess of an ion is defined as the formal charge Q of the ion considered plus the sum of the Pauling valencies, computed with respect to the other ion:

$$e^+ = Q^+ + \sum_i v_i^- \tag{4.9}$$

On the MgO(100) surface one finds for e^+

$$e^+ = 2 - \frac{5}{3} = +\frac{1}{3} \tag{4.10}$$

A negative value is computed for e^- on the oxygen anion. A positive charge excess implies Lewis acidity and a negative charge excess implies Lewis basicity. When the surface becomes exposed to NH_3, ammonia will be adsorbed to the Mg^{2+} ion. Similarly, H_2O will also bind through its oxygen atom to the surface Mg^{2+} ion.
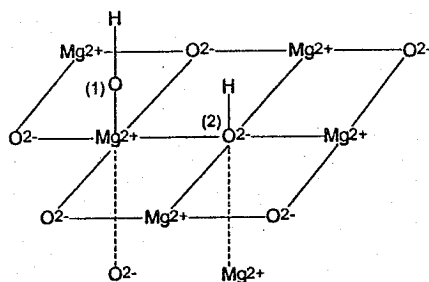
Fig. 4.57. H_2O dissociation on the MgO(100) surface.

Brønsted acidity or basicity develop when the H_2O molecule dissociates. Two different hydroxyl coordinations can develop on the MgO surface. As shown in Fig. 4.57, one hydroxyl becomes end-on coordinated to Mg^{2+}, the proton coordinates to the basic bridging oxygen anion.

To determine acidity or basicity it is useful to compute the charge excesses on oxygen atoms O(1) and O(2).

$$e(O(1)) = -2 + 1 + \frac{1}{3} = -\frac{2}{3} \tag{4.11a}$$

$$e(O(2)) = -2 + 1 + \frac{5}{3} = +\frac{2}{3} \tag{4.11b}$$

A negative excess charge implies incomplete coordination with positive charge carriers. The end-on hydroxyl group can be considered as being Brønsted basic. Oxygen atom O(2) has excess positive charge, the proton coordinated to this bridging oxygen atom behaves as a Brønsted acid. This is an important and very general conclusion.

When oxidic surfaces become exposed to water, basic hydroxyls, as well as Brønsted acidic protons, are generated upon dissociation of the water. This also occurs on the surfaces of basic oxides. There is an abundance of infrared spectroscopic information confirming the appearance of different OH groups by adsorption of HO on oxidic surfaces. Catalytic reactions induced by Brønsted acidic sites take place on such surfaces. The acidic proton is located on bridging oxygen sites.

Ammonia interacting with a surface, as sketched in Fig. 4.57, will form NH_4^+ ions coordinated to the bridging oxygen atom. Most oxide surfaces behave very similarly to the MgO surfaces. An exception is the surface generated on silica. In SiO_2 the Si cations are tetrahedrally coordinated. This coordination can be restored on the surface when the SiO_2 surface becomes exposed to H_2O. Silanol groups develop, as sketched in Fig. 4.58.

One can easily see that the excess charge on O(1) is zero. So no decision on Brønsted acidity or basicity can be made on the basis of Pauling excess charges. Chemically, the silica–silanol group is slightly acidic, due to the high charge of
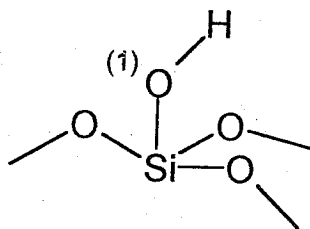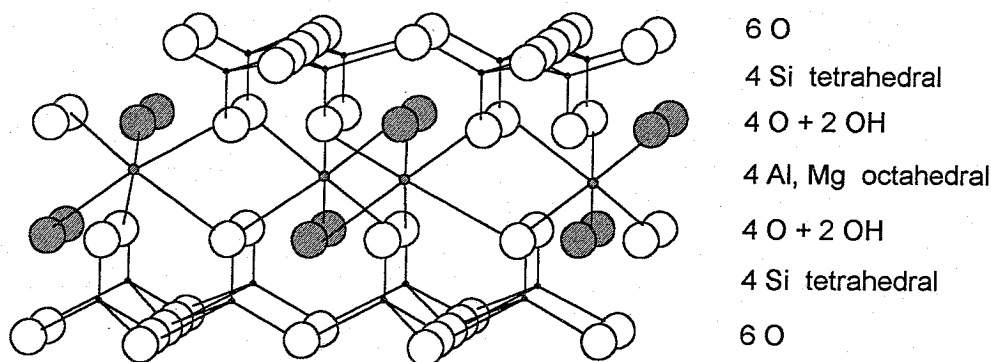
Fig. 4.58. Silanol group.

6 O

4 Si tetrahedral

4 O + 2 OH

4 Al, Mg octahedral

4 O + 2 OH

4 Si tetrahedral

6 O

Fig. 4.59. Smectite clay (schematic).

the small Si^{4+} ion to which the hydroxyl is coordinated.

Whereas the surfaces discussed so far have been generated from the bulk by a simple cut, leading to a decrease in the coordination number of the surface atoms, catalytically important acidic surfaces can also be generated in microporous or layered materials by isomorphous substitution of lattice cations. This occurs in zeolites and smectite clays. Zeolites and clays can be considered as aluminosilicates. Their lattice compositions can vary significantly. In zeolites the Al^{3+} ion can be substituted by many other trivalent cations. Si^{4+} can be partially substituted by Ti^{4+} or Ge^{4+}.

In the zeolites each lattice cation is tetrahedrally coordinated to four oxygen anions. Each oxygen anion shares two lattice cations. In smectite clays an octahedral layer, usually containing Al^{3+} or Mg^{2+}, connects two tetrahedral layers. The tetrahedral layer can be considered neutral when the tetrahedral site contains a four valent cation. This is usually a Si^{4+} ion. A top view and side view are shown in Fig. 4.59.

Isomorphous substitution of Si^{4+} by a trivalent ion (this is often an Al^{3+} ion) results in a negative lattice charge. This negative charge can be compensated by a cation located in the zeolite cage or micropore or on the clay layer. When a
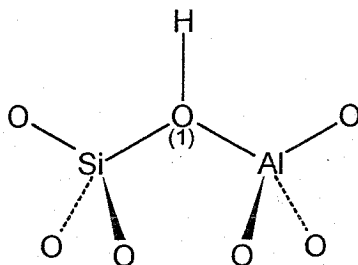
Fig. 4.60. Brønsted acidic proton.

cation is exchanged by an ammonia ion and NH_3 is subsequently desorbed, protons are generated, located on bridging oxygen atoms as sketched in Fig. 4.60.

It is interesting to compute the excess charge on the bridging oxygenation to which to protons are attached:

$$e(O(1)) = -2 + 1 + \frac{3}{4} + 1 = +\frac{3}{4} \tag{4.12}$$

Compared with (4.8b) this excess charge is quite high and indicates a strong Brønsted acidity of the attached protons.

As we saw earlier when we discussed the acidity of the silanol group, computation of charge excesses provides only a very crude estimate of acidity. As we will see for an explanation of differences in the Brønsted acidity of different zeolites, Pauling's valency rule is too crude.

The tetrahedral unit that forms the basis of the network of the zeolite makes many different structures possible. α-Quartz, the low temperature form of SiO_2, is one of the dense polymorphs. Many low-density structures can be formed, which are microporous and contain interconnected channels, bound by oxygen atoms that connect the cation-containing lattice tetrahedra. Approximately 60

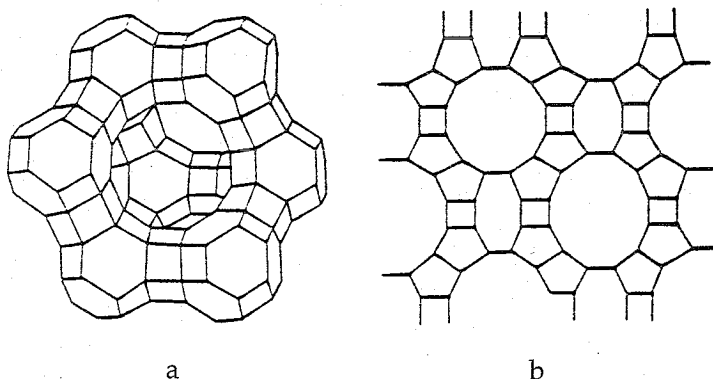a   b

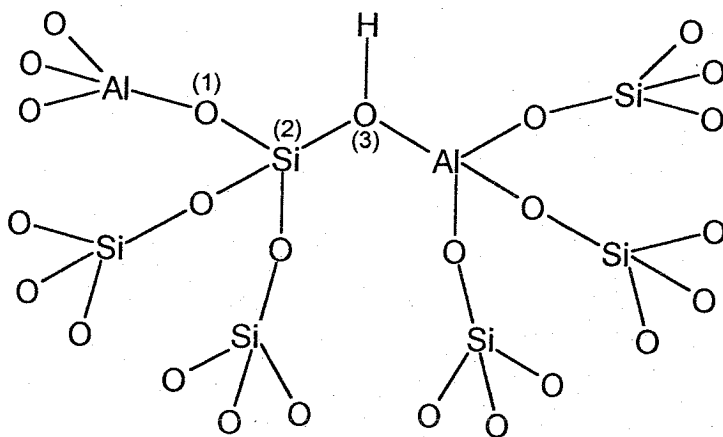Fig. 4.61. (a) Structure of faujasite. (b) Structure of mordenite.

Fig. 4.62. The second coordination shell tetrahedra with respect to a proton in a zeolite.

different structures exist; two examples of are given in Fig. 4.61a and 4.61b. The oxygen atoms are located in the middle of the lines connecting tetrahedrally coordinated atoms. The 12- or 10-ring channel openings enable organic molecules to enter the zeolite cavities.

An important factor that controls the Brønsted acidity of these catalysts is the lattice composition. For a zeolite to be Brønsted acidic, a proton has to connect two tetrahedra containing one tetravalent cation (often Si^{4+}) or a trivalent cation (often Al^{3+}). It appears that within a particular concentration region the deprotonation energy is a strong function of the Al/Si ratio.

To understand this one has to consider the cation composition of tetrahedra in the second coordination shell with respect to the proton in a zeolite (see Fig. 4.62). Because a $[TO_2]$ tetrahedron containing an Al^{3+} ion carries an overall negative charge, in zeolites no neighbouring tetrahedra can exist which both contain an Al^{3+} ion. For the [Si–O–Al] unit this implies that Al ions can only occupy the three tetrahedra next to a given silicon containing tetrahedron. The deprotonation energy is lower when the occupation by Al of the tetrahedra next to Si decreases, that is when Al is replaced by Si. Once the Al concentration has decreased so that no two [Si–O–Al] dimer pairs occur, the deprotonation energy does not vary any further with the Al content. Because of the lower charge on Al^{3+} its interaction with oxygen atoms as O(1) is less than that of a Si^{4+} ion, so that the Si atom (2) becomes more strongly bound and the bond strength between this Si atom and O(3) decreases. This strengthens the OH bond and hence increases the deprotonation energy. The generally found dependence of proton catalysed reaction on the (Al/Si) content is sketched in Fig. 4.63.

Brønsted acid-catalysed reactions will be proportional to the proton content of a zeolite as long as the intrinsic acidity of a proton remains unchanged, since the
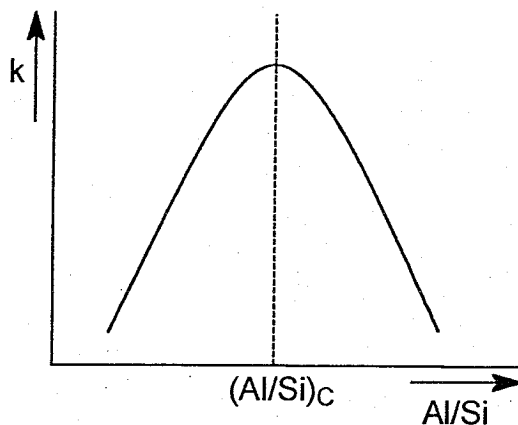
Fig. 4.63. Dependence of acid catalyzed reaction on zeolite Al/Si ratio.

proton concentration is proportional to the Al/Si ratio. Once the Al/Si ratio exceeds a critical value $(Al/Si)_c$, the intrinsic acidity of a zeolitic proton starts to decrease. This effect dominates over the increased number of protons and, as a consequence, the overall rate of the reaction decreases.

4.4.3.2 Mechanism of protonation

Protonation of a molecule creates charge separation. A positive charge is generated on the protonated molecule and a negative charge on the zeolite lattice. Charge separation is an energy-consuming process, because of the increase in potential energy. In solutions ions become stabilized by hydration or complexation with the solvent molecules. The dielectric constant of a zeolite material is low. In a zeolite the interaction between cation and negatively charged zeolite wall takes over the role of solvation of cations in liquids. The strength of the interaction with the zeolite wall depends on the cation type. The stability of a cation depends on the type of carbon atom that is protonated.

$$H_3C\overset{+}{-}CH_2 < CH_3\overset{+}{-}CH-CH_3 < CH_3\underset{+}{\overset{\overset{\textstyle CH_3}{|}}{-}C-}CH_3$$
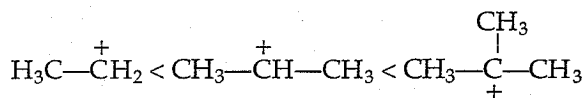
A primary carbenium ion is less stable than a secondary and a tertiary ion is most stable. The interaction of various carbenium ions with the zeolite wall decreases in the same order. A primary carbenium ion forms covalently bonded ethoxy species with the zeolite wall. As illustrated in Fig. 4.64, when an ethylene molecule approaches a proton, a weak π hydrogen bond is formed initially. Upon a proton transfer a stable σ ethoxy species is formed.
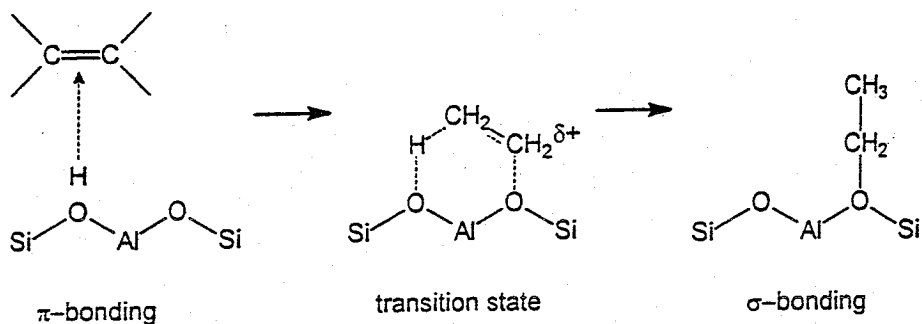
Fig. 4.64. Protonation of ethylene; π- and σ-bonded ethylene [126].

To understand differences in acidity of zeolites one has to consider not only changes in the bond strength of the OH bond, but also zeolite 'solvation' effects on the positively charged carbenium or other ions generated by protonation.

Figure 4.65 illustrates protonation of NH_3 [127,128]. Protonation proceeds via the initial formation of hydrogen-bonded NH_3, the analogue of the π complex formed with ethylene. Proton transfer only proceeds when the NH_4^+ ion can
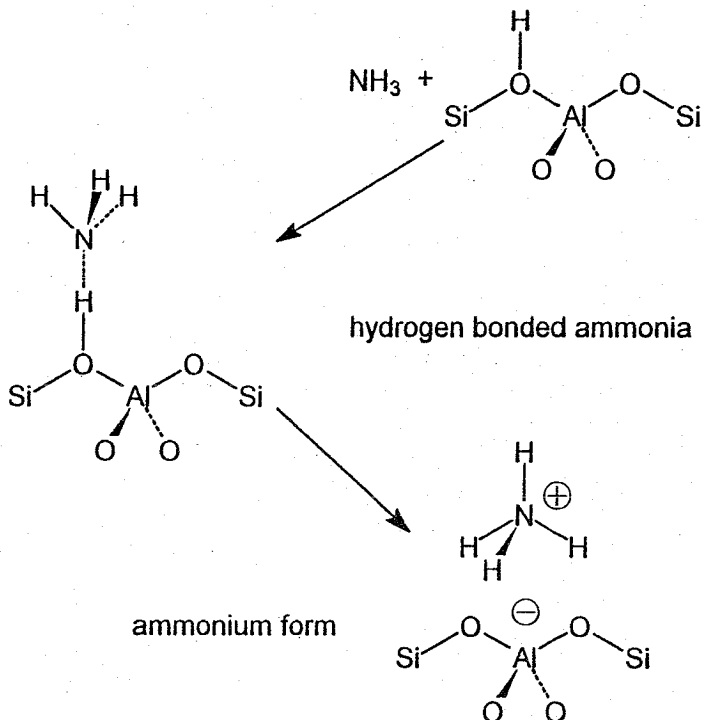
Fig. 4.65. Protonation of ammonia.

become stabilized by the negative charge on the zeolite wall. This occurs when it binds as a tri-dentate to the three negatively charged basic oxygen anion around Al^{3+}.

We also illustrate this for water protonation. The zeolite proton will attach to the water oxygen atom. The proton of water will bind to the basic lattice oxygen anion:
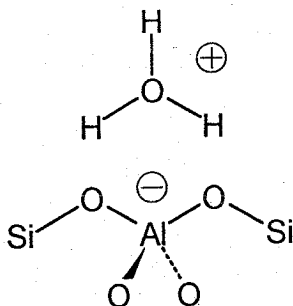
Fig. 4.66. Protonation of water.

Methanol readily gives dimethylether. The mechanism can be considered to proceed as follows:
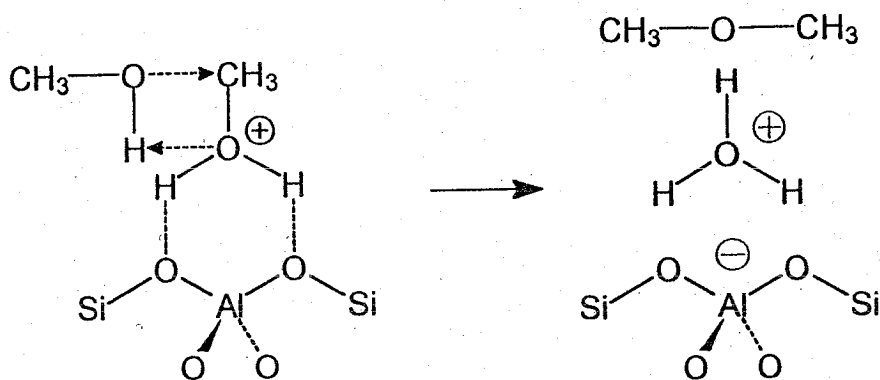
Fig. 4.67. The reaction of methanol to give dimethylether.

A key step is the formation of a stable hydronium ion upon formation of dimethylether. The concept of Brønsted acid–Lewis base catalysis also allows us to understand the formation of ethylene from methanol, as formed in zeolite-catalysed reactions. A possible mechanism is sketched in Fig. 4.68.
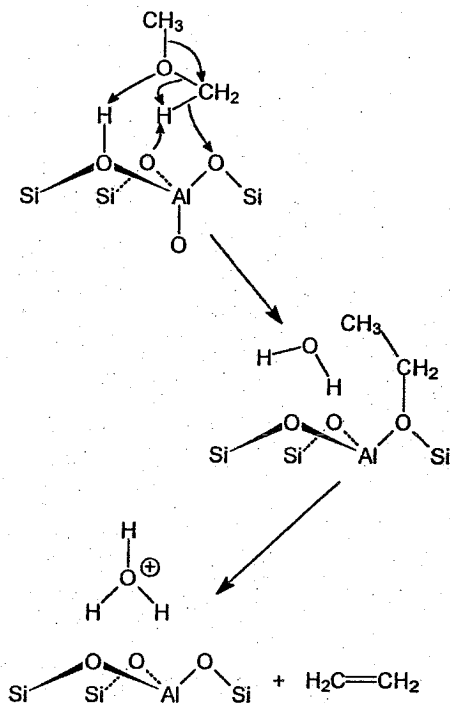
Fig. 4.68. Proton catalysed ethylene formation from dimethyl ether.

4.4.8.3 Brønsted acid-catalysed hydrocarbon activation reactions

Activation of unreactive alkanes only occurs at relatively high temperature, even with strongly acidic protons, as present in the zeolite [129]. It proceeds via the formation of carbonium ions (Fig. 4.69).
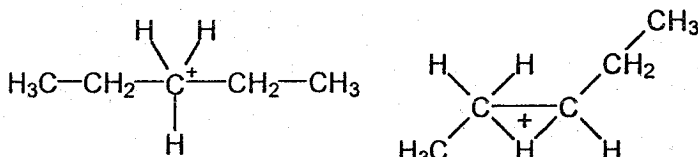
Fig. 4.69. Carbonium ions.

The carbonium ion is a nonclassical molecule, because it contains a pentacoordinated carbon atom. It is very unstable and is therefore difficult to form. It is formed at temperatures of about 500°C. Once formed it readily decomposes to a carbenium ion by H_2 formation or cracking (Fig. 4.70).

a. hydrogen formation

b. cracking

Fig. 4.70. Carbenium ion formation from carbonium ion.

Carbenium ions have been shown to isomerize readily (Fig. 4.71). As long as no primary carbenium ions are involved, isomerization of carbenium ions occurs with low activation energy and at low temperatures. Isoalkane formation occurs by reaction with another alkane and transfer of a hydride ion (Fig. 4.72).

Because the activation energy of the hydride transfer reaction is lower than that of carbonium ion formation, after a short initiation period the hydride transfer reaction will maintain the carbenium ion concentration at a steady-state level. However, secondary reactions occur that give rise to short catalyst lifetimes.

Fig. 4.71. Isomerization of carbenium ions via a triangular intermediate.

Fig. 4.72. The hydride transfer reaction.

Apart from the hydride transfer reaction the carbenium ion can undergo two other reactions. One is the cracking reaction (Fig. 4.73).

$$H_3C-\underset{\underset{CH_3}{|}}{CH}-CH_2-C^+H-CH_3 \longrightarrow H_3C-C^+H-CH_3 + H_2C=CH-CH_3$$

Fig. 4.73. β-Carbon–carbon cleavage leading to cracking.

In the cracking reaction transfer of a hydrogen atom on a β-carbon atom with respect to the ionic atom result in C–C splitting to give a smaller carbenium ion, as well as alkenes. The alkenes can undergo secondary oligomerization and polymerization reactions deactivating the catalysts. When one wishes to reduce the size of hydrocarbon molecules, the cracking reactions of Fig. 4.70 are desired. Catalytic cracking is performed on a large scale using acidic zeolite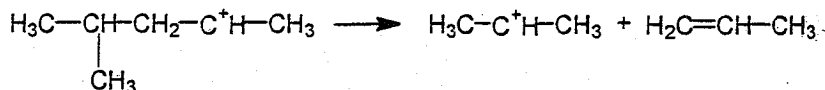s. Zeolites are preferred because the micropores of the zeolite have a shape-selective effect which prevents the alkenes from polymerizing and forming heavy molecules of large size thus rapidly deactivating the catalyst. Nonetheless the zeolites can also only be applied with short residence times and need to be regenerated frequently.

Whereas catalytic cracking is a useful reaction that requires high temperatures, a low reaction temperature is required in order to produce branched isomers at a high yield in reactions of the type shown in Fig. 4.71. The equilibrium shifts to the n-alkanes at high temperature.

In order to reduce the reaction temperature of acid catalysed alkane conversion reactions one can reduce the temperature by replacing carbonium formation by a route via the carbenium ion by protonation of alkenes generated by metal-catalysed (group 8–10 metals, e.g. Pt, Pd) dehydrogenation of alkanes. The metals can be readily dispersed in the micropores of a zeolite. A lowering of the reaction temperature is especially useful for alkane isomerization. A low temperature favours the branched product and inhibits consecutive reactions.

The reaction scheme is shown in Fig. 4.74. The reaction is performed under a high H_2 pressure in order to maintain a low alkene concentration. This is important to reduce the steady-state carbenium ion concentration on the catalyst. Once

$$H_3C-CH_2-CH_2-CH_2-CH_2-CH_3 \underset{M}{\rightleftharpoons} H_3C-CH=CH-CH_2-CH_2-CH_3$$
$$+H_2$$

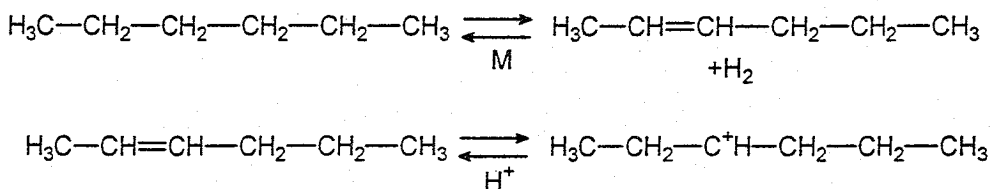$$H_3C-CH=CH-CH_2-CH_2-CH_3 \underset{H^+}{\rightleftharpoons} H_3C-CH_2-C^+H-CH_2-CH_2-CH_3$$

Fig. 4.74. Bifunctional hydroisomerization initiation scheme (see [130]).

the residence time of carbenium ions becomes too long, not only isomerization reaction will occur, but also the now undesirable cracking reaction, which is a consecutive reaction. The low alkene partial pressure reduces the carbenium ion concentration. The catalyst now performs two functions: metal-catalysed CH activation and protonation of alkenes. For this reason the hydroisomerization reaction according to Fig. 4.74 is called a bifunctional reaction.

REFERENCES

For general references to Section 4.2.1 see [1] and [2], to Section (4.2.2) see [12–14].

1   R. Hoffmann, *Solids and Surfaces*, VCH, 1988.
2   R.A. van Santen, *Theoretical Heterogeneous Catalysis*, World Scientific, 1991.
3   R.A. van Santen and A. de Koster, in L. Guczi (Editor), *New Trends in CO Activation*. Studies in Surface Science and Catalysis, Vol. 64, Elsevier, Amsterdam, 1991, p. 1.
4   R.A. van Santen, in H.H. Brongersma and R.A. van Santen (Editors), *Fundamental Aspects of Heterogeneous Catalysis Studied by Particle Beams*, NATO ASI series B265, pp. 834–112, Plenum, 1991.
5   Y. Schule, P. Siegbahn and U. Wahlgren, *J. Chem. Phys.*, 89 (1988) 6982.
6   W. Biemolt, G.J.C.S. van de Kerkhof, P.R. Davies, A.P.J. Jansen and R.A. van Santen, *Chem. Phys. Lett.*, 188 (1992) 477.
7   A. de Koster and R.A. van Santen, *J. Catal.*, 127 (1991) 141.
8   P. Sautet and J.-F. Paul, *Catal. Lett.*, 9 (1991) 3.
9   R.A. van Santen, *Progr. Surf. Sci.*, 25 (1987) 253.
10 E. Shustorovich, *Adv. Catal.*, 37 (1990) 101.
11 G.J.C. S. van de Kerkhof, W. Biemolt, A.P.J. Janssen, and R.A. van Santen, *Surf. Sci.*, in press.
12 H.B. Gray, *Electrons and Chemical Bonding*, Benjamin, New York, 1965.
13 M. Elian and R. Hoffmann, *Inorg. Chem.*, 14 (1975) 1058.
14 T.A. Albright, J.K. Burdett and M.-H. Whangbo, *Orbital Interactions in Chemistry*, J. Wiley, New York, 1985.
15 M.R.A. Blomberg and P.E.M. Siegbahn, *J. Chem. Phys.*, 78 (1983) 5689.
16 U.B. Brandemark, M.R.A. Blomberg and P.E.M. Siegbahn, *J. Phys. Chem.*, 88 (1984) 4617.
17 J.J. Low and W.A. Goddard, *J. Am. Chem. Soc.*, 106 (1984) 6928.
18 J.J. Low and W.A. Goddard, *J. Am. Chem. Soc.*, 106 (1984) 8321.
19 J.P. Collmann, L.S. Hegedus, J.R. Norton and R.G. Finke, *Principles and Applications of Organotransition Metal Chemistry*, University Science Books, Mill Valley, 1987.
20 P. Powell, *Principles of Organometallic Chemistry*, 2nd Edn., Chapman and Hall, London, 1988.
21 A. Yamamoto, *Organotransition Metal Chemistry*, Wiley, New York, 1986.
22 R. Crabtree, *The Organometallic Chemistry of the Transition Metals*, 1988.
23 C. Elschenbroich and A. Salzer, *Organometallics: A Concise Introduction*, VCH Publishers, New York, 1989.
24 J.M. Basset, J.P. Candy, A. Choplin, M. Lecomte, and A. Théolier, in R. Ugo (Editor), *Aspects of Homogeneous Catalysis*, Vol. 7, p. 87, Kluwer Academic Publishers, Dordrecht, 1990.
25 J. Falbe (Editor), *New Synthesis with Carbon Monoxide*, Springer Verlag, New York, 1980.
26 R.F. Heck and D.S. Breslow, *J. Am. Chem. Soc.*, 83 (1961) 4023.

27   F. Basolo and R.G. Pearson, *Mechanisms of Inorganic Reactions*, 2nd Edn., Wiley, New York, 1967.
28   K. Noack and F. Calderazzo, *J. Organomet. Chem.*, 10 (1967) 101.
29   R.J. Mawby, F. Basolo and R.G. Pearson, *J. Am. Chem. Soc.*, 86 (1964) 5043.
30   M.J. Calhorda, J.M. Brown and N.A.Cooley, *Organometallics*, 11 (1991) 1431.
31   N. Koga and K. Morokuma, *J. Am. Chem. Soc.*, 108 (1986), 6136.
32   J.R. Rogers, O. Kwon, and D.S. Maryneck, *Organometallics*, 10 (1991) 2816.
33   M. Brookhart and M.L.H. Green, *J. Organomet. Chem.*, 250 (1983) 395.
34   For an example of agosting interaction in the resting state of the catalyst see: M. Brookhart, A.F. Volpe, D.M. Lincoln, I.T. Horváth and J.M. Miller, *J. Am. Chem. Soc.*, 112 (1990) 5634.
35   O. Eisenstein and R. Hoffmann, *J. Am. Chem. Soc.*, 103 (1981) 4308.
36   J.W. Bruno, T.J. Marks and L.R. Morss, *J. Am. Chem. Soc.*, 105 (1983) 6842.
37   H.E. Bryndza, L.K. Fong, R.A. Paciello, W. Tam and J.E. Bercaw, *J. Am. Chem. Soc.*, 109 (1987) 1444.
38   T. Ziegler, W. Cheng, E.J. Baerends and W. Ravenek, *Inorg. Chem.*, 27 (1988) 3458.
39   L. Vaska, *Acc. Chem. Res.*, 1 (1968) 335.
40   J.K. Stille and K.S.Y. Lau, *Acc. Chem. Res.*, 10 (1977) 434.
41   C.A. Tolman, *J. Am. Chem. Soc.*, 92 (1970) 4217, 6777, 6785.
42   R.H. Crabtree, *Chem. Rev.*, 85 (1985) 245.
43   W.D. Jones and F.J. Feher, *Acc. Chem. Res.*, 22 (1989) 91.
44   G.W. Parshall, *Acc. Chem. Res.*, 8 (1975) 113.
45   G.W. Parshall, *Acc. Chem. Res.*, 3 (1970) 139.
46   G.W. Parshall, W.H. Knoth and R.A. Schunn, *J. Am. Chem. Soc.*, 91 (1969) 4990.
47   R.R. Schrock, *Acc. Chem. Res.*, 12 (1975) 98.
48   R.R. Schrock, *Organometallics*, 9 (1990) 2262.
49   T. Ito, H. Tsuchiya and A. Yamamoto, *Bull. Chem. Soc. Jpn.*, 50 (1977) 1319.
50   P.W. Jolly and G. Wilke, *The Organic Chemistry of Nickel*, Vol. II, Academic Press, New York, 1975.
51   F. Correa, R. Nakamura, R.E. Stimson, R.L. Burwell Jr. and D.F. Shriver, *J. Am. Chem. Soc.*, 102 (1980) 5112.
52   P.L. Watson and G.W. Parshall, *Acc. Chem. Res.*, 18 (1985) 51.
53   J.E. Bercaw et al. *J. Am. Chem. Soc.*, 109 (1987) 203.
54   M.S. Chinn and D.M. Heinekey, *J. Am. Chem. Soc.*, 112 (1990) 5166.
55   B.R. James, *Homogeneous Hydrogenation*, Wiley, New York, 1973.
56   A.A. Al Ammar and G. Webb, *J. Chem. Soc. Faraday Trans.*, I, 74 (1978) 195, 657; I, 75 (1979) 1900.
57   S.J. Thompson and G. Webb, *J. Chem. Soc. Chem. Commun.* (1976) 526.
58   D. Godbey, F. Zaera, R. Yates and G.A. Somorjai, *Surf. Sci.*, 167 (1986) 150.
59   S.M. Davis, F. Zaera and G.A. Somorjai, *J. Am. Chem. Soc.*, 106 (1984) 2288.
60   G.A. Somorjai and M.A. van Hove, *Adsorbate Induced Restructing of Surfaces*, US Dept. of Energy, Rept. DE-AC03-765 F00098.
61   G.A. Boreskov, *Proc. 8th ICC, Berlin, 1984*, Vol. III, p. 231, Verlag Chem., 1984.
62   N.J. Kobozev, Zhur. Fiz. Khim., 13 (1939) 1; 14 (1940) 663 and *Acta Phys. Chim.*, USSR, 9 (1938) 805.
63   D.A. Dowden in *Catalysis, Proc. 5th ICC, Miami Beach, 1972*, Vol. 1, p. 645, North Holland, 1973.
64   Y. Soma-Nota and W.M.H. Sachtler, *J. Catal.*, 34 (1974) 162.
65   W.M.H. Sachtler, *Catal. Rev. Sci. Eng.*, 14 (1976) 162.

66 T.A. Dalmon, M. Primet, G.S. Martin and B. Imelik, *Surf. Sci.*, 50 (1975) 95.

67 V. Ponec, *Adv. Catal.*, 32 (1983) 149.

68 E.H. van Broekhoven, *Progr. Surf. Sci.*, 19 (1985) 351.

69 F.J.C.M. Toolenaar, F. Stoop and V. Ponec, *J. Catal.*, 82 (1983) 1.

70 A.G.T.M. Bastein, F.J.C.M. Toolenaar and V. Ponec, *J. Catal.*, 90 (1984) 88.

71 M.J. Dees, T. Shido, Y. Iwasawa and V. Ponec, *J. Catal.*, 90 (1984) 88.

72 E.M. McCash, S.F. Parker, J. Pritchard and M.A. Chesters, *Surf. Sci.*, 215 (1989) 363.

73 J.B. Benzinger, *Appl. Sci.*, 6 (1980) 105.

74 M.Th. Karapetyants and M.K. Karapetyants, *Handbook of Thermodynamic Constants*, Ann Arbor, 1970.

75 A. de Koster and R.A. van Santen, *Surf. Sci.*, 233 (1990) 366.

76 C. Backx, C.P.M. de Groot and P. Biloen, *Surf. Sci.*, 104 (1981) 300.

77 M.A. Barteau and R.J. Madix, *Surf. Sci.*, 97 (1980) 101.

78 D.L. Thorn and R. Hoffmann, *J. Am. Chem. Soc.*, 100 (1984) 2079.

79 H. Berke and R. Hoffmann, *J. Am. Chem. Soc.*, 105 (1983) 427.

80 R. Hoffmann, *Solids and Surfaces*, VCH, 1988.

81 V. Bonacic-Kontecky, J. Kontecky, P. Fantuzci and V. Ponec, *J. Catal.*, 111, 409 (1988).

82 T. Koerts and R.A. van Santen, *Catal. Lett.*, 6 (1990) 49.

83 T. Koerts and R.A. van Santen, *J.C.S., Chem. Comm.*, 18 (1991) 1281.

84 M.J. Calhorda, J.M. Brown, N.A. Cooley, *Organometallics*, 10 (1991) 1431.

85 R. Postma, personal communication.

86 B.E. Nieuwenhuys, *Surf. Sci.*, 126 (1983) 307 and references therein.

87 N.W. Cant, P.C. Hicks and B.S. Lennon, *J. Catal.*, 54 (1978) 372.

88 J. Siera, F. Rutten and B.E. Nieuwenhuys, *Catal. Today*, 10 (1991) 353.

89 R.L. Burwell Jr., *Chem. Eng. News*, 22 (August 1966) 56.

90 R.L. Burwell Jr., *Catal. Lett.*, 5 (1990) 237.

91 C. Kemball, *Proc. Roy. Soc. (London)*, A207 (1951) 541

92 C. Kemball, *Proc. Roy. Soc. (London)*, A217 (1953) 376.

93 J.R. Anderson and C. Kemball, *Proc. Roy. Soc. (London)*, A223 (1954) 361.

94 S.B. Mohsin, M. Trenary and H.J. Robota, *J. Phys. Chem.*, 92 (1988) 5229.

95 M.A. Chesters, C. De La Cruz, P. Gardner, M. Mc Cash, P. Pudney, G. Shahid and N. Sheppard, *J. Chem. Soc. Faraday Trans.*, 86 (1990) 2757.

96 F.G. Gault, *Adv. Catal.*, 301 (1989) 1.

97 G.H. Hatkins and R.I. Masel, *Surf. Sci.*, 185 (1987) 479.

98 J.A. Gates and L.L. Kesmodel, *Surf. Sci.*, 124 (1983) 68.

99 N.R.M. Sassen, Diss. Thesis, Leiden, 1989.

100 G. Leclerq, J. Leclerq and R. Maurel, *J. Catal.*, 50 (1979) 87.

101 V. Ponec in D.A. King and D.P. Woodruff (Editors), *Chemical Physics of Solid Surfaces and Heterogeneous Catalysis*, Elsevier, 1982, Vol. 4, p. 365.

102 Z. Paal and P. Tetenyi, *React. Kin. Catal. Lett.*, 12 (1979) 131.

103 J.R. Anderson and B.G. Baker, *Proc. Roy. Soc. (London)*, A271 (1963) 402.

104 J.K.A. Clarke and J.J. Rooney, *Adv. Catal.*, 25 (1976) 125.

105 E.H. van Broekhoven and V. Ponec, *Surf. Sci.*, 162 (1985) 731.

106 J.R. Anderson and C. Kemball, *Trans. Faraday Soc.*, 51 (1955) 966.

107 J.R. Anderson and C. Kemball, *Trans. Faraday Soc.*, 51 (1955) 966.

108 G.K. Chuah, N. Kruse, W.A. Schmidt, J.H. Block and G. Abend, *J. Catal.*, 119 (1989) 342.

109 G.A. Kok, A. Noordermeer and B.E. Nieuwenhuys, *Surf. Sci.*, 135 (1982) 65.

110 R. Ryberg, *J. Chem. Phys.*, 82 (1985) 567.

111 C. Houtman and M.A. Barteau, *Langmuir*, 6 (1990) 1558.

112 J.L. Davis and M.A. Barteau, *Surf. Sci.*, 208 (1989) 383.

113 N.D.S. Canning and R.J. Madix, *J. Phys. Chem.*, 88 (1984) 2437.

114 J.B. Benziger and R.J. Madix, *Surf. Sci.*, 79 (1979) 394.

115 M.A. Henderson, Y. Zhon, J.M. White and C.A. Mims, *J. Phys. Chem.*, 93 (1989) 3688.

116 G.I. Golodets, in G. Centi and F. Trifiró (Editors), *New Developments in Selective Oxidation*, Studies in Surface Science and Catalysis, Vol. 55, Elsevier, Amsterdam, 1990, p. 693.

117 P. Mars and D.W. van Krevelen, *Chem. Eng. Sci.*, 3 (1954) 41.
    C. Kröger, *Zeit. Anorg. Allgem. Chemie*, 205 (1932) 369.

118 US Patents: 42 37070; 43 39622; 41 63761 to Texaco.

119 C.R. Adams and I.J. Jennings, *J. Catal.*, 2 (1963) 63.

120 W.M.H. Sachtler and N.H. de Boer, *Proc. 3rd ICC, Amsterdam, 1964*, North Holland Vol. 1, p. 240, 1965.

121 T.L.F. Favre, A. Maltha, P.J. Kooyman, A.P. Zuur and V. Ponec, *Proc. XI Symp. Ibero-Am. Catal.*, Guanajuato, 1988, Vol. 2, p. 807.
    J.P. Jacobs, A. Maltha, J.G.H. Reijntjes, J. Drimal, V. Ponec and H.H. Brongersma, *J. Catal.*, 147 (1994) 294.

122 J.E. Germain in M. Che and G.C. Bond (Editors), *Absorption and Catalysis on Oxide Surfaces*, Studies in Surface Science and Catalysis, Vol. 21, Elsevier, Amsterdam, 1985, p. 335.

123 J. Haber, *Proc. 8th ICC Berlin, 1984*, Chemie Verlag, 1984, Vol. 1, p. 85.

124 J.C. Volta and J.L. Portefaix, *Appl. Catal.*, 18 (1985) 1.

125 B. Grzybonska, J. Haber and J. Janas, *J. Catal.*, 49 (1977) 150.

126 V.B. Kazanskii and I.W. Senchenya, *J. Catal.*, 119 (1989) 108.

127 E.H. Teunissen, F.B. van Duyneveldt and R.A. van Santen, *J. Phys. Chem.*, 96 (1992) 366.

128 E.H. Teunissen, R.A. van Santen, A.P.J. Jansen and F.B. van Duyneveldt, *J. Phys. Chem.*, 97 (1993) 203.

129 D.M. Brouwer in R. Prins and G.C.A Schuit (Editors), *Chemistry and Chemical Engineering of Catalytic Processes*, NATO-ASIE: 39, Sijthoff and Noordholt, Alphen aan de Rijn, 1980, p. 137.

130 P.A. Jacobs and J.A. Martens in H. van Bekkum, E.M. Flanigen and J.C. Jansen (Editors), *Introduction to Zeolite Science and Practice*, Studies in Surface Science and Catalysis, Vol. 58, Elsevier, Amsterdam, 1991, p. 445.